Basics of Magnetism

A. K. Majumdar

Ramakrishna Mission Vivekananda University, Belur

Indian Institute of Technology, Kanpur (1972-2006)
S. N. Bose National Centre for Basic Sciences, Kolkata (2006-2011)
Indian Institute of Science Education & Research Kolkata (2011-2013)

A School on Basics of Magnetism and Investigations of Magnetic Properties of Materials using Synchrotron Radiation, March 24–28, 2014,
Raja Ramanna Centre for Advanced Technology, Indore

Plan of the lectures (Ambitious???)

History of Magnetism

Diamagnetism

Paramagnetism

Ferromagnetism

Weiss' "molecular field" theory

Heisenberg's theory

Bloch's Spin-wave theory

Band theory

Magnetic anisotropies

Ferromagnetic domains

Magnetism(Contd.)

Indirect exchange: RKKY, Super-exchange, Spin glass

R & D in Magnetic Materials after 1973

Magnetoresistance (MR)/(OMR)/(AMR)

Giant magnetoresistance (GMR)/Spin-valve structure

Tunnel magnetoresistance (TMR)

Colossal magnetoresistance (CMR)

Nano-magnetism/ Superparamagnetism

History of Magnetism

The study of magnetism started with the discovery of the ***Lodestone (or Magnetite Fe_3O_4)*** around 500-800B.C. in Greece & China.

Lodestones attract pieces of iron and the attraction can only be stopped by placing between them an iron plate, which acts as a ***Magnetic Shield.***

The directional property of the ***Lodestone*** was utilized to design ***"Compass",*** which was invented around 100A.D. in China.

Theoretical understanding of magnetism came ***only*** in the 19^{th} century along with some basic applications .

Diamagnetism

Diamagnetism

The weakest manifestation of magnetism is ***Diamagnetism*** $\Rightarrow$

Change of orbital moment of electrons due to applied magnetic fields.

The relevant parameter which quantifies the strength of magnetism is the ***Magnetic Susceptibility,*** χ, which is defined as

$$\chi = Lt_{H \to 0} (dM/dH).$$

Diamagnetism arises from two basic laws of Physics, viz.,

Faraday's law & Lenz's law:

An electron moves around a nucleus in a circle of radius, r.

A magnetic field **H** is applied. The induced electric field, **E(r),** generated during the change is

$$E(r)\, 2\pi r = -(1/c)\, d/dt\, (H \pi r^2)$$

$$\text{or, } E(r) = -(r/2c)\, dH/dt.$$

Diamagnetism

This E(r) produces a force & hence a torque = – e E(r) r

= dL/dt = (e r^2 /2c) dH/dt, (e > 0).

The extra ΔL(L was already there for the orbital moion) due to the turning of the field = (e r^2 /2) H.

The corresponding moment μ= - (e/2mc) ΔL = (e^2 r^2 /4mc^2) H, $r^2 = x^2 + y^2$.

For N atoms per unit volume with atomic no. Z, the ***Magnetic Susceptibility***

$$\chi = -(Ne^2Z\langle r^2\rangle_{av})/6mc^2.$$

QM treatment also produces the same answer!!!

χ is ***negative*** ≈ - 10^{-6} in cgs units in the case of typical diamagnetic materials. In SI units it is - 4π x 10^{-6}.

Diamagnetism

QM treatment

The Hamiltonian of a charged particle in a magnetic field **B** is

$H = (\mathbf{p} - e\mathbf{A}/c)^2/2m + e\varphi$, **A =** vector pot, φ = scalar pot, valid for both classical & QM.

K.E. is not dependent on **B**, so it is unlikely that **A** enters H. ***But***

$\mathbf{p} = \mathbf{p}_{kin} + \mathbf{p}_{field} = m\mathbf{V} + e\mathbf{A}/c$ (C. Kittel, ***ISSP (7th Ed.)*** App. G, P: 654)

& K.E. $= (m\mathbf{v})^2/2m = (\mathbf{p} - e\mathbf{A}/c)^2/2m$, where $\mathbf{B} = \nabla \times \mathbf{A}$.

So, **B**-field-dependent part of H is $ieh/4\pi mc[\nabla . \mathbf{A} + \mathbf{A}.\nabla] + e^2 A^2/2mc^2$.(1)

Diamagnetism

QM treatment

If **B** is uniform and II z-axis, $A_X = -\frac{1}{2} y B$, $A_Y = \frac{1}{2} x B$, and $A_Z = 0$.

So, (1) becomes $H = ieh/4\pi mc(x\,\partial/\partial y - y\,\partial/\partial x) + e^2B^2/8mc^2(x^2 + y^2)B$.

$\downarrow$ $\downarrow$

$L_Z \Rightarrow$ Orbital PM $E' = e^2B^2/12mc^2 \langle r^2 \rangle$ by 1st order perturbation theory.

$M = -\partial E'/\partial B = -(Ne^2Z\langle r^2\rangle_{av})/6mc^2\, B$ for N atoms/volume with atomic no. Z.

Since B = H for non-magnetic materials

$$\chi = Lt_{H\to 0}\,(dM/dH) = -(Ne^2Z\langle r^2\rangle_{av})/6mc^2 \text{ independent of T}$$

- **M(T) shows negative and temperature independent magnetization.**

Diamagnetism

Example: Calculate the diamagnetic susceptibility of a mole of atomic hydrogen.

Ground state wave-function of hydrogen is $\Psi = 1/(\pi a_0^3)^{1/2} \exp(-r/a_0)$ where a_0= Bohr radius. If $|0\rangle$ is the ground state wave-function

$$\langle r^2\rangle_{av} = \langle 0|r^2|0\rangle = \int \Psi^* r^2 \Psi \, d^3r = 1/(\pi a_0^3) \int \exp(-2r/a_0)\, r^2\, 4\pi r^2\, dr$$

$$= (4/a_0^3)\,(a_0/2)^5 \int_0^\infty x^4\, e^{-x}\, dx = (4/a_0^3)\,(a_0/2)^5\, 4! = 3a_0^2 \text{ (Putting } 2r/a_0 = x).$$

$\chi = -(Ne^2Z\langle r^2\rangle_{av})/6mc^2$. For hydrogen Z = 1, taking N as the Avogadro number, for a mole of hydrogen $\chi = -Ne^2a_0^2/2mc^2$

Some applications:

- Meissner effect in a superconductor: χ as high as – 1 below T_C
  - perfect diamagnetism to make B = 0 ***inside*** (flux expulsion) below H_{C1}.
- Substrates of present day magnetic sensors are mostly diamagnetic like Si, sapphire, etc.

Paramagnetism

Atoms/molecules in solids/liquids with odd no of electrons($S \neq 0$):

free Na atoms with partly filled inner shells, metals (Pauli), etc.

contribute to **electron** paramagnetism.

Free atoms/ions with partly filled inner shells, e.g., Mn^{2+}, Gd^{3+}, U^{4+}

show **ionic** paramagnetism.

A collection of magnetic moments, **m**, interact with external magnetic field **H**:
Interaction energy $U = - \mathbf{m} . \mathbf{H}$.

Magnetization results from the orientation of the magnetic moments but thermal disorders disturb this orientation.

The energy levels, according to quantum mechanics, of an assembly of

N magnetic ions/vol., each of spin **S** and a Lande factor of g in a magnetic field of H_0, is given by $\varepsilon_m = g \mu_B m H_0$ where $-S \leq m \leq +S$.

Partition function $Z = \Sigma_m \exp(- g \mu_B m H_0/k_B T) = \Sigma_m \exp(- m x)$

where $x = g \mu_B H_0/k_B T$, μ_B = Bohr magneton = $eh/(2\pi)2mc$.

$$Z = \sinh\{(2S+1)x/2\}/\sinh(x/2)$$

Paramagnetism

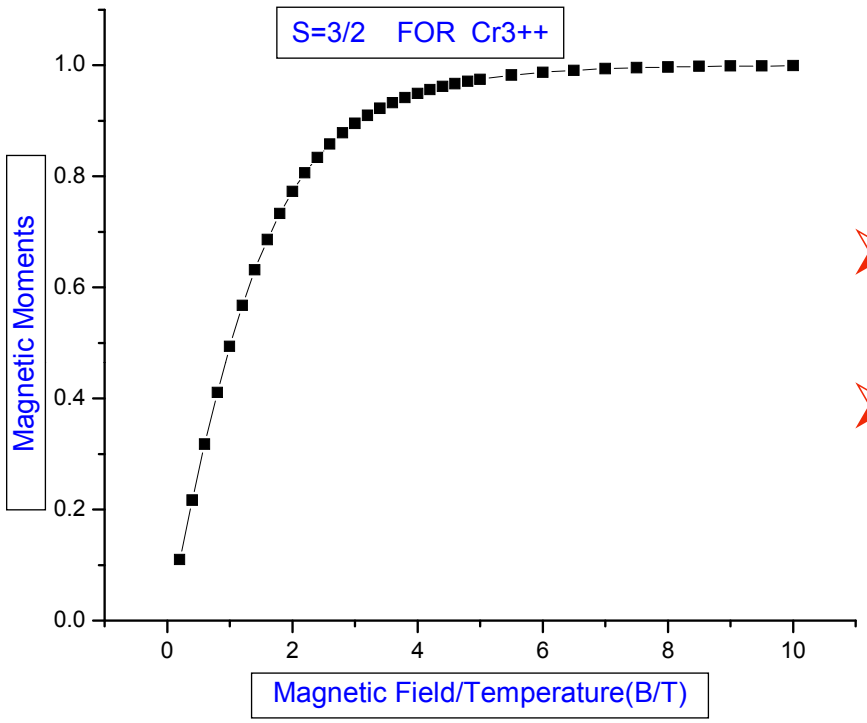

- In this <m> vs. H/T plot paramagnetic saturation is observed only at very high H & low T, i.e. x >>1when ***coth x → 1 and < m > →*** $Ng\mu_B S$.
- At 4 K & 1tesla, <m> ~ 14 % of its saturation value.
- For ordinary temperature like 300 K & 1 T field, x <<1. Then ***coth x → 1/x + x/3*** and so

$$<m> \rightarrow \left(\frac{g\mu_B S(S+1)}{3k_B T}\right)H \qquad Ng\mu_B.$$

Thus <m> varies linearly with field.

< m > = $Ng\mu_B S$[coth X- 1/X] = L(X) = Langevin function when S → ∞ , X = Sx.

Paramagnetism

So the ***Magnetic Susceptibility,*** χ at temperature T is

$$\chi = (N g^2 \mu_B^2 S(S+1)/3k_B)*1/T$$
$$= C/T,$$

where **N**= No. of ions/vol, ***g*** is the Lande factor, μ_B is the Bohr magneton and ***C*** is the ***Curie constant.*** This is the famous

Curie law for paramagnets.

Some applications:

To obtain temperatures lower than 4.2 K, paramagnetic salts like, $CeMgNO_3$, $CrKSO_4$, etc., are kept in an isothermal 4.2 K bath & a field of, say, 1 T applied.

>>> Entropy of the system decreases & heat goes out. Finally the magnetic field is removed adiabatically.

>>> Lattice temperature drops to mK range.

Similarly microkelvin is obtained using nuclear demagnetization.

Paramagnetism

Rare–earth ions

Fascinating magnetic properties, also quite complex in nature:
Ce58: [Xe] $4f^2\ 5d^0\ 6s^2$, Ce^{3+} = [Xe] $4f^1\ 5d^0$ since $6s^2$ and $4f^1$ removed
Yb70: [Xe] $4f^{14}\ 5d^0\ 6s^2$, Yb^{3+} = [Xe] $4f^{13}\ 5d^0$ since $6s^2$ and $4f^1$ removed
Note: [Xe] = [Kr] $4d^{10}\ 5s^2\ 5p^6$
In trivalent ions the outermost shells are identical $5s^2\ 5p^6$ like neutral Xe.

In La (just before RE) 4f is empty, Ce^{+++} has one 4f electron, this number increases to 13 for Yb and $4f^{14}$ at Lu, the radii contracting from 1.11 Å (Ce) to 0.94 Å (Yb) → ***Lanthanide Contraction.*** The number of 4f electrons compacted in the inner shell with a radius of 0.3 Å is what determines the magnetic properties of these RE ions. The atoms have a (2J+1)-fold degenerate ground state which is lifted by a magnetic field.

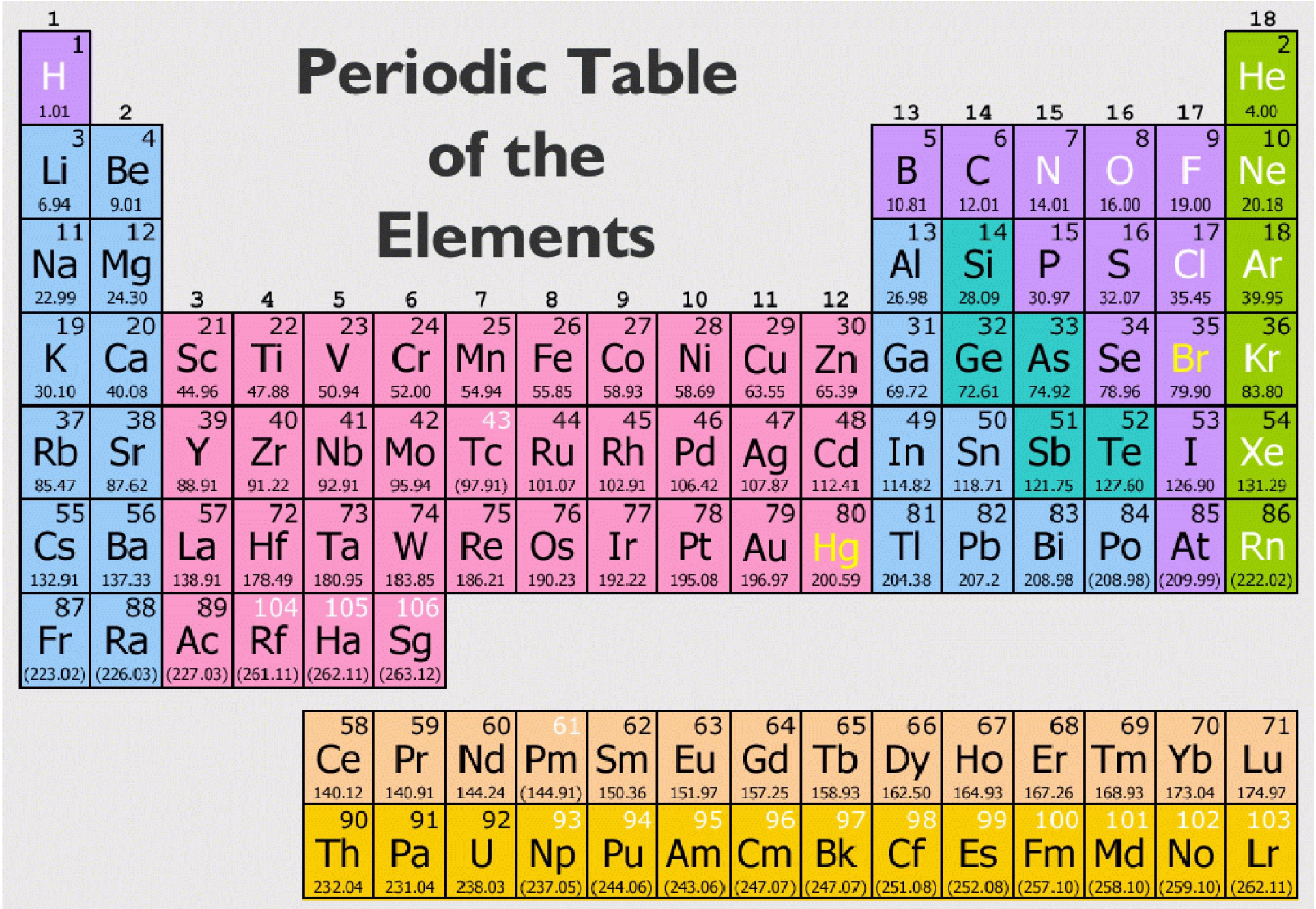
Periodic Table of the Elements
1
18
2
13
14
15
16
17
3
4
5
6
7
8
9
10
11
12
1 H 1.01
2 He 4.00
3 Li 6.94
4 Be 9.01
5 B 10.81
6 C 12.01
7 N 14.01
8 O 16.00
9 F 19.00
10 Ne 20.18
11 Na 22.99
12 Mg 24.30
13 Al 26.98
14 Si 28.09
15 P 30.97
16 S 32.07
17 Cl 35.45
18 Ar 39.95
19 K 30.10
20 Ca 40.08
21 Sc 44.96
22 Ti 47.88
23 V 50.94
24 Cr 52.00
25 Mn 54.94
26 Fe 55.85
27 Co 58.93
28 Ni 58.69
29 Cu 63.55
30 Zn 65.39
31 Ga 69.72
32 Ge 72.61
33 As 74.92
34 Se 78.96
35 Br 79.90
36 Kr 83.80
37 Rb 85.47
38 Sr 87.62
39 Y 88.91
40 Zr 91.22
41 Nb 92.91
42 Mo 95.94
43 Tc (97.91)
44 Ru 101.07
45 Rh 102.91
46 Pd 106.42
47 Ag 107.87
48 Cd 112.41
49 In 114.82
50 Sn 118.71
51 Sb 121.75
52 Te 127.60
53 I 126.90
54 Xe 131.29
55 Cs 132.91
56 Ba 137.33
57 La 138.91
72 Hf 178.49
73 Ta 180.95
74 W 183.85
75 Re 186.21
76 Os 190.23
77 Ir 192.22
78 Pt 195.08
79 Au 196.97
80 Hg 200.59
81 Tl 204.38
82 Pb 207.2
83 Bi 208.98
84 Po (208.98)
85 At (209.99)
86 Rn (222.02)
87 Fr (223.02)
88 Ra (226.03)
89 Ac (227.03)
104 Rf (261.11)
105 Ha (262.11)
106 Sg (263.12)
58 Ce 140.12
59 Pr 140.91
60 Nd 144.24
61 Pm (144.91)
62 Sm 150.36
63 Eu 151.97
64 Gd 157.25
65 Tb 158.93
66 Dy 162.50
67 Ho 164.93
68 Er 167.26
69 Tm 168.93
70 Yb 173.04
71 Lu 174.97
90 Th 232.04
91 Pa 231.04
92 U 238.03
93 Np (237.05)
94 Pu (244.06)
95 Am (243.06)
96 Cm (247.07)
97 Bk (247.07)
98 Cf (251.08)
99 Es (252.08)
100 Fm (257.10)
101 Md (258.10)
102 No (259.10)
103 Lr (262.11)

Paramagnetism

Rare–earth ions

In a Curie PM

$$\chi = \frac{NJ(J+1)g^2\mu_B^2}{3\kappa_B T} = \frac{C}{T} = \frac{Np^2\mu_\beta^2}{3\kappa_B T},$$

where p = effective Bohr Magnetron number

$$= g\left[J(J+1)\right],$$

g = Lande factor $= 1 + \dfrac{J(J+1) + S(S+1) - L(L+1)}{2J(J+1)}$.

'p' calculated from above for the RE^{3+} ions using Hund's rule agrees very well with experimental values except for Eu^{3+} & Sm^{3+}.

Paramagnetism

Hund's rules

Formulated by Friedrich Hund, a German Physicist around 1927.
The ground state of an ion is characterized by:

1. Maximum value of the total *spin* S allowed by Pauli's exclusion principle.

2. Maximum value of the total *orbital* angular momentum L consistent with the total value of S, hence PEP.

3. The value of the *total* angular momentum J is equal to $|L-S|$ when the shell is less than half full & $|L+S|$ when the shell is more than half full.

When it is just half full, the first rule gives L = 0 and so J = S.

Paramagnetism

Explanation 1st rule: It's origin is Pauli's exclusion principle and Coulomb repulsion between electrons.

↑↑ are separated more and hence have less positive P.E. than for

↑↓ electrons. Therefore, all electrons tend to become ↑↑ giving maximum S.

Explanation of 2nd rule: Best approached by model calculations.

Example of rules 1 & 2: $Mn^{2+}: Mn\ 3d^5 4s^{2'}\ Mn^{2+}\ \ 3d^5$ (half- filled 3d sub shell)

All 5 spins can be ‖ to each other if each electron occupies a different orbital and there are exactly 5 orbitals characterized by orbital angular quantum nos. m_l = -2, -1, 0, 1, 2. One expects S = 5/2 and so $\sum m_l = 0$. Therefore **L** is 0 as observed.

Paramagnetism

Explanation of 3rd rule:

Consequence of the sign of the spin-orbit interaction. For a single electron, energy is lowest when **S** is antiparallel to **L** (**L.S** = - ve). But the low energy pairs m_l and m_s are progressively used up as one adds electrons to the shell. By PEP, when the shell is more than half full the state of lowest energy necessarily has the **S** ‖ **L**.

Examples of rule 3:

Ce^{3+} = [Xe] $4f^1\ 5s^2\ 5p^6$ since $6s^2$ and $4f^1$ removed. Similarly Pr^{3+} = [Xe] $4f^2\ 5s^2\ 5p^6$. Nd^{3+}, Pm^{3+}, Sm^{3+}, Eu^{3+},Gd^{3+},Tb^{3+}, Dy^{3+}, Ho^{3+},Er^{3+} ,Tm^{3+},Yb^{3+} have $4f^3$ to $4f^{13}$. Take Ce^{3+}: It has one 4f electron, an f electron has l = 3, S = ½, **4f shell is less than half full** (full shell has 14 electrons), by third rule = **J** = $|\mathbf{L} - \mathbf{S}|$ = L - 1/2 = 5/2.

Spectroscopic notation ${}^{2s+1}L_J \Rightarrow {}^{2}F_{5/2}$ [L = 0, 1, 2, 3, 4, 5, 6 are S, P, D, F, G, H, I].

Pr^{3+} has 2 '4f' electrons: S = 1, l = 3. Both cannot have m_l = 3 (PEP),

so max. L is not 6 but 5. **J** = $|\mathbf{L} - \mathbf{S}|$ = 5 -1 = 4. $\Rightarrow$ ***${}^3H_4$***

Paramagnetism

Nd^{3+} has 3 '4f' electrons:S = 3/2 (first rule), l = 3 → m_l = 3, 2, 1, 0, -1, - 2, - 3. L = $\sum m_l = 6$, J = 6 - 3/2 = 9/2 ⇒ $^4I_{9/2}$

Pm^{3+} has 4 '4f' electrons: S = 2, L = 6, J = L - S = 4 ⇒ $^5I_4$

Exactly ½ full 4f shell: : Gd^{3+} has 7 '4f' electrons; S = 7/2, L = 0, J = 7/2

⇒ $^8S_{7/2}$

4f shell is more than half full: Ho^{3+} has 10 '4f' electrons: 7 will be ↑,

3 will be ↓. S = 2, L = 6 [3 2 1 0 -1 -2 -3] ; J = 6 + 2 = 8 ⇒ $^5I_8$ and so on.

Note: 4f shell is well within the inner core (localized) surrounded by $5s^2$, $5p^6$, and $6s^2$ & so almost unaffected by crystal field (CF). 3d transition element ions, being in the outermost shell, are affected by strongly inhomogeneous electric field, called the "crystal field" (CF) of neighboring ions in a real crystal. **L-S** coupling breaks, so states are **not** specified by **J**. (2L + 1) degenerate levels for the free ions may split by the CF and **L** is often quenched. **"p" calculated from J gives total disagreement with experiments.**

For details see C. Kittel, ISSP (7th Ed.) P. 423-429; Ashcroft & Mermin, P. 650-659.

3d transition element ions

Details: If **E** is towards a fixed nucleus, classically all L_X, L_Y, L_Z are constants (fixed plane for a central force). In QM L_Z & L^2 are constants of motion but in a non-central field (as in a crystal) the orbital plane is not fixed & the components of **L** are not constants & may be even zero on the average. If $\langle L_Z \rangle = 0$, **L** is said to be quenched.

In an orthorhombic crystal, say, the neighboring charges produce about the nucleus a potential $V = Ax^2 + By^2 - (A + B)z^2$ satisfying Laplace equation & the crystal symmetry. For L =1, the orbital moment of all 3 energy levels have $\langle L_Z \rangle = 0$. The CF splits the degenerate level with separation >> what the B-field does. For cubic symmetry, there is no quadratic term in V & so p electron levels will remain triply degenerate unless there is a ***spontaneous*** displacement of the magnetic ion, called ***Jahn-Teller effect***, which lifts the degeneracy and lowers its energy.

Mn^{3+} has a large JT effect in manganites which produces Colossal Magnetoresistance (CMR).

For details see C. Kittel, ISSP (7th Ed.) P. 425-429; Ashcroft & Mermin, P. 655-659.

Van Vleck Paramagnetism

Examples: EuO, EuF, EuBO where CW-law fails.

If an atomic or molecular system has no moment in the ground state,

$$\left|\langle 0 | m_s | 0 \rangle\right| = 0$$

Suppose a non-diagonal matrix element <s|m_s|0> of the magnetic moment operator connecting the ground state $|0\rangle$ to the excited state $\langle s| \neq 0$.

Then 2nd order perturbation theory gives the perturbed GS wave function

$\Psi_0' = \Psi_0 + \left(B/\Delta\right)\langle s|m_s|0\rangle\Psi_S$ in the weak-field approximation $\mu_s B << \Delta$,

where $\Delta = E_s - E_0$. Similarly for the ES $\Psi_S' = \Psi_S - \left(B/\Delta\right)\langle 0|m_s|s\rangle\Psi_0$.

Perturbed GS has a moment $\langle o'|m_s|o'\rangle \sim +2B\left|\langle s|m_s|o\rangle\right|^2/\Delta$.

Perturbed ES has a moment $\langle s'|m_s|s'\rangle \sim -2B\left|\langle s|m_s|o\rangle\right|^2/\Delta$.

Excess population in GS (with $x = \Delta/k_BT$) = N[(exp(x)-1)/(exp(x)+1)]

Case 1. High-T: $\Delta << k_BT$, $x \rightarrow 0$, Excess ~ Nx/2 = N $\Delta/2k_BT$

Van Vleck Paramagnetism

Resultant magnetization is $M = \frac{2B\left|\langle s|m_s|0\rangle\right|^2}{\Delta}\frac{N\Delta}{2k_BT}$

& $\chi = \underset{\beta\to 0}{Lt}\frac{dM}{dB} = N\left|\langle s|m_s|0\rangle\right|^2 / k_BT = \frac{C}{T}$, N = no. of molecules/volume.

Looks like a Curie paramagnet. The magnetization here is connected to the field-induced electronic transition whereas for free spins (Curie) M is due to the redistribution of ions among the 2S+1 spin states. It is independent of Δ.

Case 2. Low-T: $\Delta >> k_BT$ $\quad x \to \infty$, Excess $\to$ N

Here the population is nearly all in the ground state and

$$M = \frac{2NB\left|\langle s|m_s|0\rangle\right|^2}{\Delta}$$ [no $\frac{\Delta}{2k_BT}$ fraction here] and

$$\chi = \frac{2N\left|\langle s|m_s|0\rangle\right|^2}{\Delta}$$, independent of T.

(just like a diamagnet but with + ve χ, hence a PM).

C. Kittel, ISSP (7th Ed.) P. 430.

Pauli Paramagnetism

Pauli paramagnetism in metals

Paramagnetic susceptibility of a free electron gas: There is a change in the occupation number of up & down spin electrons even in a non-magnetic metal when a magnetic field B is applied.

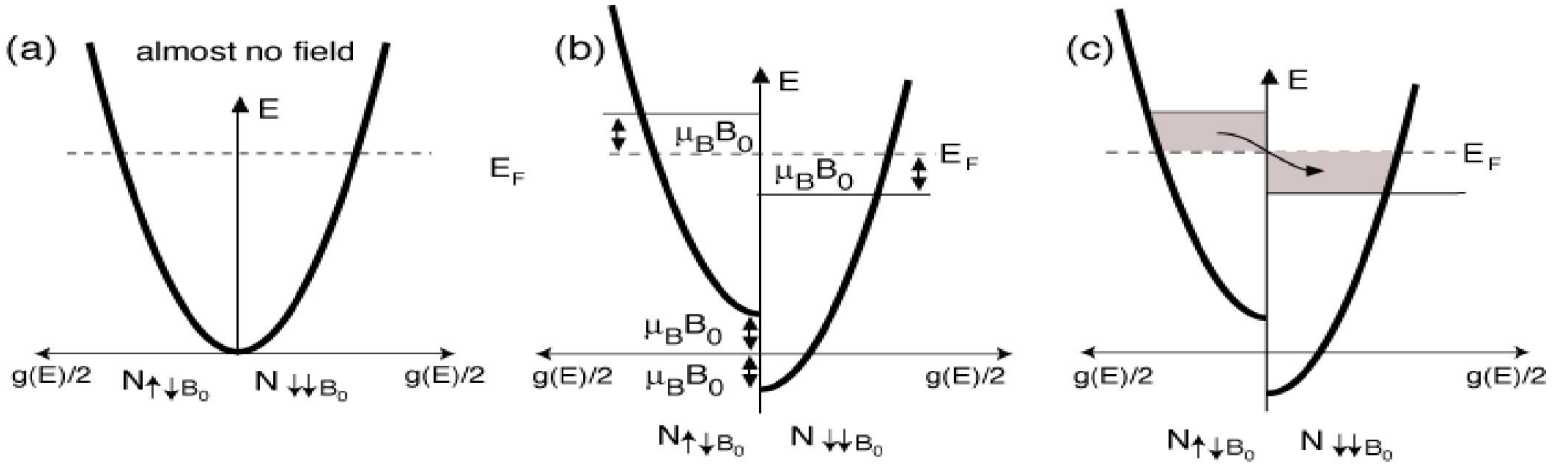

The magnetization is given by ($T << T_F$)

$$M = \mu (N_{up} - N_{down}) = \mu^2 \, D(\varepsilon_F) \, B, \; D(\varepsilon_F) = 3N/2\varepsilon_F.$$

$$\therefore \chi = 3 N \mu^2 / 2\varepsilon_F, \text{ independent of temperature,}$$

where $D(\varepsilon_F)$ = Density of states at the Fermi level ε_F.

Ferromagnetism

Any theory of ferromagnetism has to explain:

i) Existence of spontaneous magnetization **M** below $\mathbf{T_C}$ (Paramagnetic to ferromagnetic transition temperature).

ii) Below T_C, a small $\mathbf{H_0}$ produces $\mathbf{M_S}$ from M ~ 0 at H = 0.

There are three major theories on ferromagnetism:

1. Weiss' "molecular field" theory

2. Heisenberg's theory

3. Bloch's spin-wave theory ($T << T_C$).

R. M. Bozorth, A survey of the theory of ferromagnetism, Rev. Mod. Phys. 17, No. 1 (1945).

Ferromagnetism

Weiss' "molecular field" theory

Weiss proposed that:

i) Below **TC** spontaneously magnetized domains, randomly oriented give M ~ 0 at H = 0. A small $\mathbf{H_0}$ produces domain growth with $\mathbf{M} \parallel \mathbf{H_0}$.

ii) A very strong "molecular field", H_E of unknown origin aligns the atomic moments within a domain.

Taking alignment energy ~ thermal energy below Tc,

For Fe: $H_E = k_B T_C / \mu \sim 107$ gauss $\sim 10^3$ T !!!

$$E_{d\text{-}d} \sim [\mu_1 . \mu_2 - (\mu_1 . r_{12})(\mu_2 . r_{12})]/4\pi\varepsilon_0 r^3 .$$

Classical dipole-dipole interaction gives a field of ~ 0.1 T only & is anisotropic but ferromagnetic anisotropy is only a second order effect.

So ???

Weiss postulated that $H_E = \lambda M$, where λ is the molecular field parameter and M is the saturation magnetization.

Ferromagnetism

Curie-Weiss law

Curie theory of paramagnetism gave

$M = [(N g^2 \mu_B^2 S(S+1)/3k_B)*1/T]*H$

$= (C/T)*H.$

Replacing H by $H_0 + \lambda M$ we get

$M = CH_0/(T-C\lambda)$

$\therefore \chi = C/(T-T^*_C),$

where $T^*_C = C\lambda$ = paramagnetic Curie temperature.

Putting g ~ 2, S = 1, M = 1700 emu/g

one gets $\lambda = 5000$ & $H_E = 10^3$ T for Fe.

This theory fails to explain χ (T) for

$T < T^*_C$.

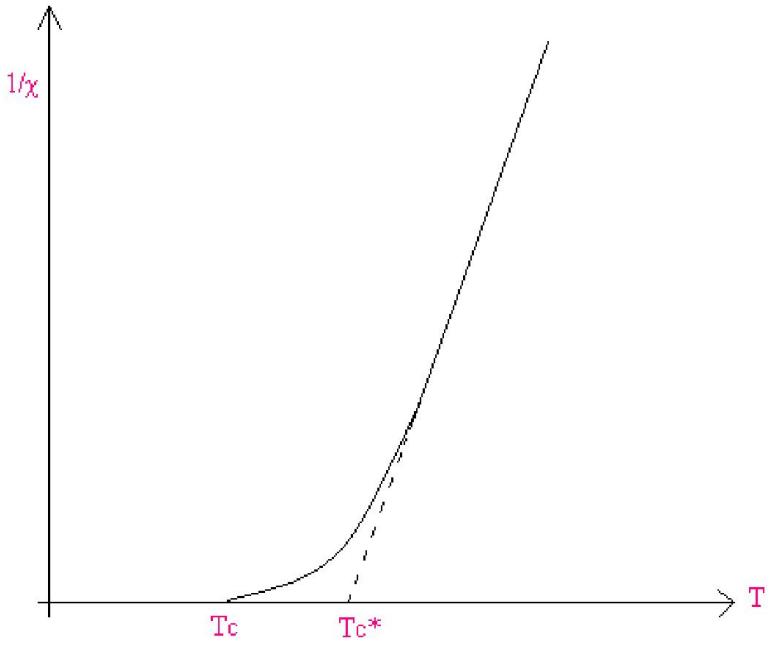

Ferromagnetism

Temperature Dependence of Saturation Magnetization below Curie Temperature (T_C)

Using molecular field approximation

Magnetization $M = Ng\mu_B [(S+1/2)\coth(S+1/2)x) - 1/2\coth(x/2)]$

$= Ng\mu_B F_S(x)$ (1) with $x = g\mu_B H_0/k_B T$.

In ferromagnetism, $M \neq 0$ even when $H_0 = 0$. So, here $x = g\mu_B \lambda M/k_B T$.

Or, $M = k_B Tx/g\mu_B \lambda$. (2) Its slope determined by temperature T.

The point of intersection, P of (1) & (2) gives M at a given T.

At T = 0, $M = Ng\mu_B S$. As T increases P → lower values of M till T_C is reached beyond which M = 0. This happens

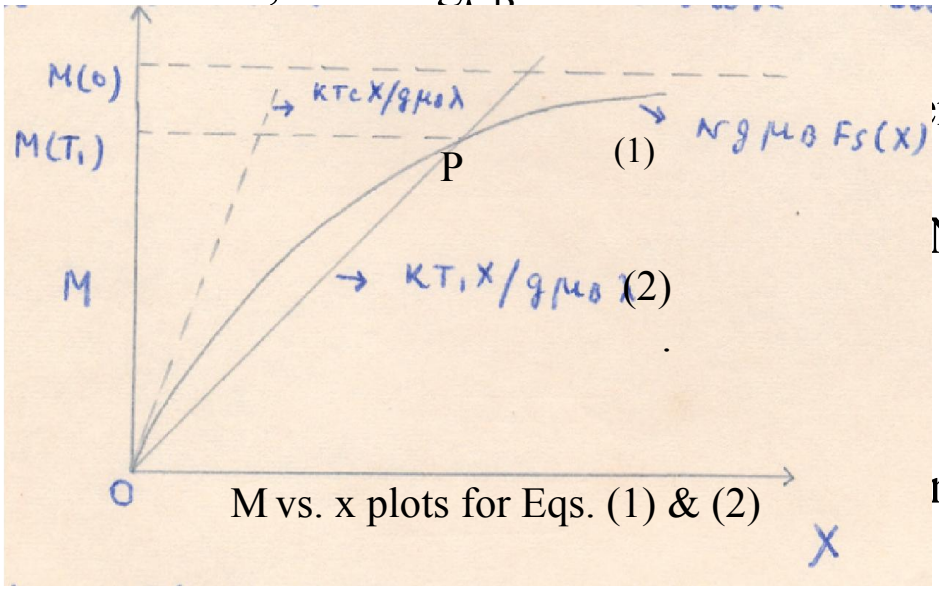

M vs. x plots for Eqs. (1) & (2)

n slopes of (1) & (2) at x = 0 are

, $M = Ng\mu_B S(S+1)x/3$.

$Ng\mu_B S(S+1)/3 = k_B T_C/g\mu_B \lambda$.

Thus $T_C = \lambda N g^2 \mu_B^2 S(S+1)/3k_B = T_C^*$.

Expts. show (See slide 23) that the

netic Curie temp. $T_C^* \sim 3$-5 %

Ferromagnetism

Low-temperature Magnetization at $T << T_C$

Here $x = g\mu_B \lambda M/k_B T >> 1$(very large) & $\coth x \sim 1 + 2 \exp(-2x)$.

$$M = Ng\mu_B [(S+1/2)\coth(S+1/2)x) - 1/2\coth(x/2)]$$
$$\sim Ng\mu_B [(S+1/2)(1+ 2 \exp(-2(S+1/2)x)) - ½(1+2\exp(-x))]$$
$$\sim Ng\mu_B S[1 - 1/S \exp(- g\mu_B \lambda M(0)/k_B T)].$$

Since $\lambda = T_C/C$ and $C = Ng^2 \mu_B^2 S(S+1)/3k_B$

$$M(T)/M(0) = 1- (1/S) \exp[-(3/(S+1))(T_C/T)] \sim 1 - e^{-1/T}$$

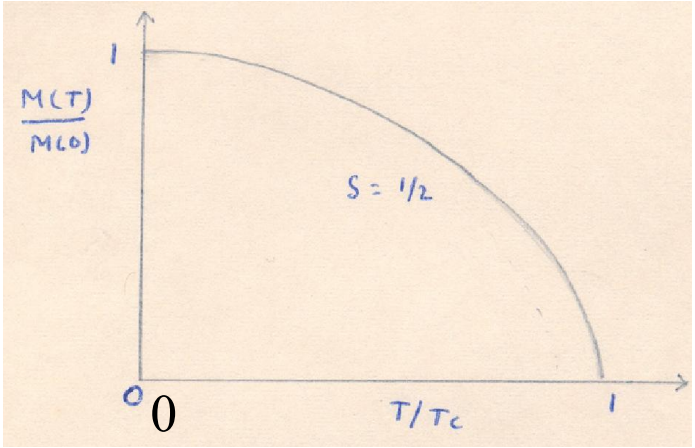

Experiments show that the above exponential variation, as shown, holds good for $T/T_C > 0.5$ but at lower temperatures it is a power-law variation instead. This discrepancy is very well explained by Bloch's spin-wave theory.

Ferromagnetism

Heisenberg's Theory (Exchange effect)

The origin of the molecular field was unknown to Weiss.

Heisenberg found the origin of Weiss' "molecular field" in the "quantum mechanical exchange effect", which is basically electrical in nature. Electron spins on the same or neighboring atoms tend to be coupled by the exchange effect – a consequence of Pauli's Exclusion Principle (PEP). If u_i and u_j are the two wave-functions into which we "put 2 electrons", there are two types of states that we can construct according to their having antiparallel or parallel spins. These are

$$\Psi(\mathbf{r}_1, \mathbf{r}_2) = 1/\sqrt{2}\,[u_i(\mathbf{r}_1)\,u_j(\mathbf{r}_2) \pm u_j(\mathbf{r}_1)\,u_i(\mathbf{r}_2)],$$

where ± correspond to space symmetric/antisymmetric (spin singlet, S = 0/spin triplet, S=1) states.

Singlet: spin anisymmetric: S = 0: $(\uparrow\downarrow - \downarrow\uparrow)/\sqrt{2}$, m = 0.

Triplet: spin symmetric: S = 1: $\uparrow\uparrow$ m = 1; $\downarrow\downarrow$ m = -1;

$(\uparrow\downarrow + \downarrow\uparrow)\sqrt{2}$, m = 0.

Ferromagnetism

Also, if you exchange the electrons between the two states, i.e., interchange r_1 and r_2, $\Psi(-)$ changes sign but $\Psi(+)$ remains the same. If the two electrons have the same spin($\|$), they cannot occupy the same **r**. Thus $\Psi(-) = 0$ if $\mathbf{r}_1 = \mathbf{r}_2$. Now if you calculate the average of the Coulomb energy $e^2/|\mathbf{r}_{12}|$ in these two states we find them different by

$$J_{ij} = \int u_i^*(\vec{r}_1) u_j^*(\vec{r}_2) \frac{e^2}{|\vec{r}_i - \vec{r}_j|} u_j(\vec{r}_1) u_i(\vec{r}_2) d\vec{r}_1 d\vec{r}_2 \quad (1)$$

which is the "exchange integral".

Exchange Hamiltonian

In a 2-electron system (hydrogen molecule) we have to use antisymmeteric (AS) total wave-function due to PEP. Thus the spatial wave-function must be either symmetric (S) [singlet] or AS [triplet] corresponding to AS or S spin functions. The energy is given by

$$E = K_{ij} \pm J_{ij}, \qquad (2)$$

where +/- sign corresponds to S/AS spatial wave functions.

K_{ij} is a combination of kinetic and potential energy integrals while J_{ij} is the exchange integral given by Eq. (1) above. J_{ij} can be shown to be positive for well-behaved functions.

Ferromagnetism

$\mathbf{S}_i$ & $\mathbf{S}_j$ are two spins at the lattice sites i and j (one valence electron/atom).

$$\mathbf{S}_{i+j} = \mathbf{S}_i + \mathbf{S}_j, \qquad S_{i+j}^2 = S_i^2 + S_j^2 + 2\,\mathbf{S}_i.\,\mathbf{S}_j,$$

$$s_{i+j}(s_{i+j}+1) = s(s+1) + s(s+1) + 2\,\mathbf{S}_i.\,\mathbf{S}_j.$$

$s_{i+j} = 0$ (singlet) and 1(triplet), $s\,(s+1) = ¾$.

Therefore, the eigenvalue of $2\,\mathbf{S}_i.\,\mathbf{S}_j = -3/2$ (singlet) and 1/2 (triplet)
and hence that of $½ + 2\,\mathbf{S}_i.\,\mathbf{S}_j = -1$ (singlet) and +1 (triplet).

Thus, Eq.(2) can be thought of as the eigenvalue of a "spin Hamiltonian"

$$H_{ij} = K_{ij} - (½ + 2\,\mathbf{S}_i.\,\mathbf{S}_j)\,J_{ij}.$$

So, the "exchange Hamiltonian" is taken as

$$H_e = -2\,\mathbf{S}_i.\,\mathbf{S}_j\,J_{ij}. \qquad (3)$$

We have omitted $-½\,J_{ij}$ since it does not depend on spin orientation & hence does not play any role in magnetism. H_e is isotropic, in agreement with experiments showing ferromagnetic anisotropy (dipole-dipole interaction) as a second-order effect.

Ferromagnetism

- Heisenberg gave the exchange Hamiltonian the form which is isotropic. $H_e = -2J_{ij}\vec{S}_i.\vec{S}_j$
- In the presence of a field H_0, the Hamiltonian becomes

$$H = -g\mu_B H_0 \sum_i S_i^Z - 2\sum_{\substack{i,j \\ i\neq j}} J_{ij}\vec{S}_i.\vec{S}_j$$

Assuming nearest neighbour exchange interaction, $J_{ij} = J$ & $\mathbf{S_i} = \mathbf{S}$

we get the Hamiltonian $H = -g\mu_B H_0 NS - \frac{1}{2}\{2JNZ(S)^2\} = -MH_0 - JNZ(S)^2$

where Z = no. of N.N's, N = no. of atoms/vol, $M = Ng\mu_B S$. The 1st term is due to the external field while the second is due to the Weiss field H_E. So, H can also be written as $H = -M(H_0 + \frac{1}{2} H_E)$.

Simple algebra gives using $T_C = C\lambda$, $C = N g^2 \mu_B^2 S(S+1)/3k_B$ in $H = -M(H_0 + \frac{1}{2} H_E)$,

$\lambda = (2JZ/Ng^2\mu_B^2)$ & $J = (3k_B T_C/2ZS(S+1)) \sim 12$ meV for Fe with S = 1.

Taking S = ½ , one gets $(k_B T_C/ ZJ) = 0.5$ from mean-field theory

Ferromagnetism

Bloch's Spin-wave Theory (T << Tc)

In the ground state of a FM (at 0 K) the atoms at different lattice sites have their maximum z-component of spin, $S_j^z = S$.

As T increases the system is excited out of its ground state giving rise to sinusoidal ***"Spin Waves",*** as shown below.

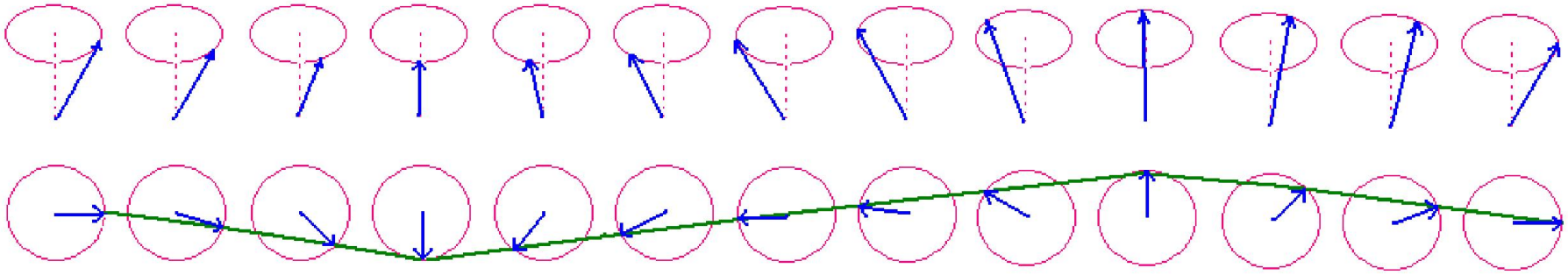

- The amplitude of this wave at j^{th} site is proportional to $S-S_j^z$.
- The energy of these spin waves is quantized and the energy quantum is called a ***"magnon".***

Ferromagnetism

Considering nearest neighbour interaction and Zeeman energy, the Hamiltonian is written as

$$\mathrm{H} = -\mathrm{J}\sum_{\mathrm{j},\delta} \vec{S}_{\mathrm{j}} \,.\, \vec{S}_{\mathrm{j}+\delta} - g\mu_B H_0 \sum_{j} S_j^Z \,, \qquad (18)$$

where δ is a vector joining j^{th} atom to its nearest neighbours.
The total spin and its z-component, i.e.,

$$\mathbf{S}^2 = \left(\sum_{\mathrm{j}} \vec{S}_{\mathrm{j}}\right)^2 \quad \& \quad \mathbf{S}^{\mathrm{Z}} = \sum_{\mathrm{j}} \mathrm{S}_{\mathrm{j}}^{\mathrm{Z}} \quad \text{are constants of motion.}$$

In the ground state all spins are parallel:

$$\therefore \quad \vec{\mathbf{S}} = N\vec{S} \,,$$

$$\therefore \mathbf{S}^2 \,|0> = NS(NS+1)|0>; \quad \mathbf{S}^Z \,|0> = NS\,|0>.$$

Ferromagnetism

The spin-waves are treated as quantized particles subject to creation and annihilation operators for Bosons. The spin deviation operator is defined as $\eta_j = S - S_j^Z$.
The eigenstates Ψ of H in (18) satisfying $H\Psi = E\Psi$ can be expanded in terms of the eigenstates of these spin deviation operators as

$$\Psi = \sum_{n_1, \ \ldots \ ,n_N} b(n_1, \ \ldots \ , n_N) \ \varphi_{n_1, \ \ldots \ ,n_N}$$

where $\eta_j \ \varphi_{n_1, \ \ldots \ ,n_N} = n_j \ \varphi_{n_1, \ \ldots \ ,n_N}$

Here n_j is the eigenvalue of the spin deviation operator η_j of the j^{th} atom.

Ferromagnetism

The next 9 slides could be summarized as follows:

The spin raising and lowering operators $S_j^{\pm} = S_j^x \pm i\, S_j^y$ operate on the eigenstates of the spin deviation operator η_j. The spin raising operator raises the z-component of the spin and hence lowers the spin deviation and vice-versa. Then one defines Boson creation (a_j^+) and annihilation (a_j) operators as well as the number operator ($a_j^+ a_j$) in terms of $S_j^{\pm}$ and S_j^z**.** These relations are called Holstein-Primakoff transformation. Then one makes a transformation of $S_j^{\pm}$ and S_j^z in terms of magnon creation and annihilation operators, b_k^+ and b_k. **K** is found from the periodic boundary condition. $b_k^+ b_k$ is the magnon number operator with eigenvalue n_k for the magnon state **K.**

Finally, the energy needed to excite a magnon in the state K, in the case of a simple cubic crystal of nearest neighbor distance "a" is

$$(h/2\pi)\omega_k = g\, \mu_B\, H_0 + 2\, J\, S\, a^2\, k^2.$$

This is the magnon dispersion relation where $E \sim k^2$ like that of free electrons.

Ferromagnetism

The spin raising and lowering operators are defined as usual

$$S_j^{\pm} = S_j^x \pm i\, S_j^y \tag{19}$$

We know from the theory of angular momentum that

$$S_j^+ \varphi_{n_j} = \sqrt{\left(S - S_j^Z\right)\left(S + S_j^Z + 1\right)}\ \varphi_{n_j - 1}$$

$$S_j^- \varphi_{n_j} = \sqrt{\left(S + S_j^Z\right)\left(S - S_j^Z + 1\right)}\ \varphi_{n_j + 1} \tag{20}$$

It is to be noticed that the spin raising operator raises the Z-component, i.e., it lowers the spin deviation of & vice versa.

Boson creation and annihilation operators are defined as

Ferromagnetism

$$a_j^+ \varphi_{n_j} = \sqrt{n_j + 1}\ \varphi_{n_j+1}$$

$$a_j \varphi_{n_j} = \sqrt{n_j}\ \varphi_{n_j-1} \qquad (21)$$

satisfying the commutation relation

$$\left[a_j , a_{j'}^+\right] = \delta_{jj'}$$

The number operator $\eta_j = a_j^+ a_j = S - S_j^Z$

From (19), (20) and (21) we can deduce,

$$S_j^+ = (2S)^{1/2} \left(1 - \frac{a_j^+ a_j}{2S}\right)^{1/2} a_j \qquad (22)$$

$$S_j^- = (2S)^{1/2}\, a_j^+ \left(1 - \frac{a_j^+ a_j}{2S}\right)^{1/2} \qquad (23)$$

$$S_j^Z = S - a_j^+ a_j \qquad (24)$$

Eqs. (22)-(24) are known as Holstein-Primakoff transformation.

Ferromagnetism

It is better to transform a_j^+, a_j (atomic) to the spin-wave variable b_K^+ , b_K as

$$b_k = \frac{1}{\sqrt{N}} \sum_j e^{i\vec{K}.\vec{R}_j} \; a_j \quad ; \quad b_k^+ = \frac{1}{\sqrt{N}} \sum_j e^{-i\vec{K}.\vec{R}_j} \; a_j^+ \; ,$$

where $\mathbf{R}_j$ is the position vector of the j[th] atom. The inverse transformation gives

$$a_j = \frac{1}{\sqrt{N}} \sum_K e^{-i\vec{K}.\vec{R}_j} \; b_k \quad ; \quad a_j^+ = \frac{1}{\sqrt{N}} \sum_K e^{i\vec{K}.\vec{R}_j} \; b_k^+ . \qquad (25)$$

The subscript K's are all vectors.

Ferromagnetism

It is easy to show that,

$$[b_K , b_{K'}^{+}] = \delta_{KK'}$$

b_K^{+} is the magnon creation operator while b_K is the magnon annihilation operator. The K-values are determined from periodic boundary condition.

Now we want to express S_j^{+}, S_j^{-}, & S_j^{Z} in terms of b_K's and consider only low lying energy levels for which

$$\langle a_j^{+} a_j \rangle / S = \langle n_j \rangle / S \ll 1 \qquad (26)$$

This means almost all the spins are lined in the same direction (low temperature). Under condition (26) we can expand (22), (23) & (24) and substitute the a_j's by b_K's from (25).

$$S_j^{+} = (2S)^{\frac{1}{2}} \left[a_j - a_j^{+} a_j a_j / 4S + \ldots \right]$$

$$= \frac{(2S)^{\frac{1}{2}}}{\sqrt{N}} \left[\sum_K e^{-i \vec{K}.\vec{R}_j} \; b_K - (4SN)^{-1} \sum_{K,K',K''} e^{-i(\vec{K}-\vec{K}'-\vec{K}'').\vec{R}_j} \; b_K^{+} b_K b_{K''} + \cdots \right]$$

Ferromagnetism

$$S_j^- = (2S)^{\frac{1}{2}} \left[a_j^+ - a_j^+ a_j^+ a_j / 4S + \ \ldots\right]$$

$$= \frac{(2S)^{\frac{1}{2}}}{\sqrt{N}} \left[\sum_K e^{i\,\vec{K}.\vec{R}_j}\ b_K^+ - (4SN)^{-1} \sum_{K,K',K''} e^{i(\vec{K}+\vec{K}'-\vec{K}'').\vec{R}_j}\ b_K^+\, b_{K'}^+\, b_{K''} + \cdots\right]$$

$$S_j^Z = S - a_j^+ a_j \ \ = S - N^{-1} \sum_{K,K'} e^{i(\vec{K}-\vec{K}').\vec{R}_j}\ b_K^+\, b_{K'} + \cdots$$

The spin deviation operator for the whole system is

$$\sum_j S - \sum_j S_j^Z = NS - \sum_j S_j^Z = \sum_j a_j^+\, a_j$$

$$= N^{-1} \sum_{K,K'} e^{i(\vec{K}-\vec{K}').\vec{R}_j} \ \ b_K^+\ b_{K'} = \sum_K b_K^+\, b_K$$

Thus, $\quad S^Z = NS - \sum_K b_K^+\, b_K \qquad (27)$

Ferromagnetism

Just as $a_j^+ a_j$ is the Boson number operator with eigenvalue n_j , $b_K^+ b_K$ is magnon number operator with eigenvalue n_K for the magnon state K.

Dispersion realation for magnons:

Substituting S_j^+, S_j^-, & S_j^Z in (18) we get,

$$H = -J \sum_{j,\delta} \left[\frac{1}{2} S_j^+ S_{j+\delta}^- + \frac{1}{2} S_j^- S_{j+\delta}^+ + S_j^Z S_{j+\delta}^Z \right] - g\mu_B H \sum_j S_j^Z$$

For Z-nearest neighbour, considering only terms bilinear in spin variables

$$= -JNZS^2 - \left(\frac{JS}{N}\right) \sum_{j\delta K\, K'} \left[e^{-i(\vec{K}-\vec{K}').\vec{R}_j} e^{i(\vec{K}'.\vec{\delta})}\, b_K\, b_{K'}^+ \right.$$

$$\left. + e^{i(\vec{K}-\vec{K'}).\vec{R}_j}\; b_K^+ b_{K'} \quad e^{-i(\vec{K}'.\vec{\delta})} - e^{i(\vec{K}-\vec{K}').\vec{R}_j}\; b_K^+ b_{K'} \right.$$

Ferromagnetism

$$- e^{i\left(\vec{K}-\vec{K}'\right).\left(\vec{R}_j+\vec{\delta}\right)}\ b_K^+ b_{K'}\Big] - g\mu_B H_0 NS$$

$$+ g\frac{\mu_B}{N} H_0 \sum_{jKK'} e^{i\left(\vec{K}-\vec{K}'\right).\ \vec{R}_j}\ b_K^+ b_{K'}$$

Summing over j gives, (using $\delta_{KK'} = \frac{1}{N}\sum_j e^{i\left(\vec{K}-\vec{K}'\right).\ \vec{R}_j}$)

$$H = -JNZS^2 - \left(\frac{JS}{N}\right)\sum_{\delta K}\Big[Ne^{i\left(\vec{K}.\vec{\delta}\right)}\ b_K\ b_K^+$$

$$+ N\ \ e^{-i\left(\vec{K}.\vec{\delta}\right)}\ b_K^+ b_K\ - N\ \ b_K^+ b_K - N\ b_K^+ b_K\Big]$$

$$- g\mu_B H_0 NS + \ g\frac{\mu_B}{N} H_0 \sum_K N\ \ b_K^+ b_K$$

Ferromagnetism

Introducing $\gamma_K = \frac{1}{Z}\sum_{\delta} e^{i\vec{K}.\vec{\delta}}$ (28)

$$H = -JNZS^2 - g\mu_B H_0 NS - JSZ\sum_K \left[\gamma_K\, b_K\, b_K^+ + \gamma_{-K}\, b_K^+ b_K - 2\, b_K^+ b_K\right] + g\mu_B H_0 \sum_K b_K^+ b_K$$

With a centre of symmetry $\gamma_K = \gamma_{-K}$

$$H = -JNZS^2 - g\mu_B H_0 NS - 2SZJ\sum_K [b_K^+ b_K(\gamma_K - 1)] - JSZ\sum_K \gamma_K + g\mu_B H_0 \sum_K b_K^+ b_K$$

$\left[\because \sum_K \gamma_K = 0\right]$

Ferromagnetism

Or,
$$H = -JNZS^2 - g\mu_B H_0 NS + 2SZJ\sum_K [(1-\gamma_K)\, n_K] + g\mu_B H_0 \sum_K n_K$$
$$H_0' = \sum_K \hbar\omega_K\, n_K = 2SZJ\sum_K [(1-\gamma_K)\, n_K] + g\mu_B H_0 \sum_K n_K \qquad (29)$$

where H_0' = energy above ground state. The ground state energy $H_{G\text{-}S}$ is

$$H_{G-S} = -JNZS^2 - g\mu_B H_0 NS$$

$$\varepsilon_K = \hbar\omega_K = 2SZJ(1-\gamma_K)\, n_K + g\mu_B H_0 \qquad (30)$$

For $\left|\vec{K}.\vec{\delta}\right| \ll 1$

$$\hbar\omega_K = g\mu_B H_0 + JS\sum_\delta (\vec{K}.\vec{\delta})^2$$

For cubic system $\hbar\omega_K = g\mu_B H_0 + 2JS\, a^2\, K^2$ (31)

is the magnon dispersion relation.

Ferromagnetism

Temperature dependence of magnetization

Let us calculate the magnetization as a function of temperature using the magnon dispersion relation (31) and see whether it predicts the correct behaviour at low temperatures or not. The molecular field theory, by the way, failed at low temperatures.

The number of spin waves of all modes excited at a temperature T in thermal equilibrium is given by Bose-Einstein statistics

$$n = \sum_K \langle n_K \rangle = \sum_K \frac{1}{e^{\hbar\omega_K / k_\beta T} - 1} \ ,$$

where k_β = Boltzmann constant and the summation extends over all values of K in the first Brillouin zone allowed by periodic boundary condition. Changing summation to integration

$$n = \int_0^{\omega_{max}} \frac{D(\omega)d\omega}{e^{\hbar\omega/k_\beta T} - 1} \ , \qquad (32)$$

where D (ω) dω = the no. of magnons between frequency ω and ω + dω .

If g (K) = density of states in K-space/vol.

Ferromagnetism

$$D(\omega)d\omega = g(\text{k})d^3k = \frac{1}{(2\pi)^3}\, 4\pi\, k^2 \frac{dk}{d\omega} d\omega$$

Putting $H_0 = 0$ in the dispersion relation (31) we get

$$\varepsilon_K = \hbar\omega_K = \; 2JS\, a^2\, K^2 \quad (33)$$

$$K^2 \frac{dK}{d\omega} = \; K^2 \; \frac{\hbar}{4JSKa^2} = \frac{1}{2}\left(\frac{\hbar}{2JSa^2}\right)^{3/2} \; \omega^{1/2}$$

$$D(\omega)d\omega = \frac{1}{4\pi^2}\left(\frac{\hbar}{2JSa^2}\right)^{3/2} \; \omega^{1/2} d\omega$$

At low temperatures $k_\beta T << \hbar\omega_{max}$ and so we can replace the upper limit by $\propto$

If $x = \hbar\omega/k_\beta T$

$$n = \frac{1}{4\pi^2}\left(\frac{k_\beta T}{2JS\, a^2}\right)^{3/2} \int_0^{\propto} \frac{x^{1/2} dx}{e^x - 1} = \frac{1}{4\pi^2}\left(\frac{k_\beta T}{2JS\, a^2}\right)^{3/2} \xi(3/2)\, \Gamma(3/2)$$

$\xi\left(3/2\right)\Gamma\left(3/2\right) = 0.0587\ (4\pi^2)$ from integral tables

$$n = 0.0587 \times \left(\frac{k_\beta T}{2JSa^2}\right)^{3/2} \quad (34)$$

Ferromagnetism

Each spin wave changes the total S by one unit of $\hbar$ from (27)

$$S^Z = NS - \sum_K b_K^+ b_K = NS - \Sigma_k \langle n_K \rangle = NS - n$$

$$= NS - 0.0587 \left(\frac{k_\beta T}{2JSa^2} \right)^{3/2} \qquad \text{From (34)}$$

The saturation magnetization at a temperature T is given by

$$M_S(T) = g\mu_B S^Z = g\mu_B [NS - 0.0587 \left(\frac{k_\beta T}{2JSa^2} \right)^{3/2}]$$

Now $M_S(0) = g\mu_B NS$

Fractional change of magnetization

$$\frac{M_S(0) - M_S(T)}{M_S(0)} = \frac{\Delta M}{M_S(0)} = \frac{0.0587}{NSa^3} \left(\frac{k_\beta T}{2JS} \right)^{3/2}$$

Ferromagnetism

For cubic symmetry N = no. of atoms/volume = Q/a^3 where Q = 1, 2, 4 for simple, body-centred & face-centred cubic, respectively.

$$\frac{\Delta M}{M_S(0)} = \frac{0.0587}{QS}\left(\frac{k_\beta T}{2JS}\right)^{3/2}. \qquad (35)$$

This is known as <u>Bloch's $T^{3/2}$ law.</u>

To analyse experimental data it is conventional to write (35) in the form

$$\frac{M_S(T)}{M_S(0)} = 1 - \left\{0.0587\ \frac{g\mu_B}{M_S(0)}\left(\frac{k_\beta T}{2JSa^2}\right)^{3/2}\right\} T^{3/2}$$

$$= 1 - C_{3/2} T^{3/2}.$$

Ferromagnetism

Specific heat contribution from magnons:

Another simple but interesting consequence of the dispersion relation is the magnon contribution to specific heat. The internal energy / unit volume is in thermal equilibrium is given by (following the previous arguments)

$$U = \frac{1}{4\pi^2}\left(\frac{\hbar}{2JSa^2}\right)^{3/2}\int_0^{\omega_{max}} \frac{\omega^{3/2}\,d\omega}{e^{\hbar\omega/k_\beta T}-1}$$

$$= \frac{1}{4\pi^2}\left(\frac{\hbar}{2JSa^2}\right)^{3/2}\hbar\left(\frac{k_\beta T}{\hbar}\right)^{5/2}\int_0^{\propto}\frac{x^{3/2}dx}{e^x-1}$$

$$= \frac{1}{4\pi^2}\left(\frac{k_\beta}{2JSa^2}\right)^{3/2} k_\beta T^{5/2}\,\xi(5/2)\,\Gamma(5/2) \qquad \left[\because \xi\left(5/2\right)\Gamma\left(5/2\right) = 0.045\,(4\pi^2)\right]$$

$$C_V = \left(\frac{\partial U}{\partial T}\right)_V = \frac{1}{4\pi^2}\left(\frac{k_\beta T}{2JSa^2}\right)^{3/2} k_\beta\,\frac{5}{2}\times 4\pi^2 \times 0.045$$

$$\boxed{C_V = 0.1125\,k_\beta\left(\frac{k_\beta T}{2JSa^2}\right)^{3/2}} \qquad (36)$$

Ferromagnetism

Thus spin wave theory of ferromagnetism explains quite well the experimental observation on temperature dependence of magnetization and the specific heat contribution of magnons at low temperatures.

References used:

1. C. Kittel, Quantum Theory of Solids, 1972.
2. C. Kittel, "Low-temperature Physics", Lectures delivered at Les Houches, 1961.
3. J. Van Vleck, " A survey of the Theory of Ferromagnetism", Review of Modern Physics, 17, No. 1, 1945.

Ferromagnetism

Summary of spin-wave theory

- Using the spin-wave dispersion relation for a cubic system

  $(h/2\pi)\omega_k = g\mu_B H_0 + 2Jsa^2k^2$,

  one calculates the number of magnons, n in thermal equilibrium at temperature T to be proportional to $T^{3/2}$ and hence

  $M(T) = M(0)\,[1 + A_Z\{3/2, T_g/T\}\,T^{3/2} + B_Z\{5/2, T_g/T\}T^{5/2}]$.

  This is the famous Bloch's $T^{3/2}$.

- Similarly specific heat contribution of magnons is also ~ $T^{3/2}$.

- Both are in very good agreement with experiments.

  [C. Kittel, Quantum Theory of Solids]

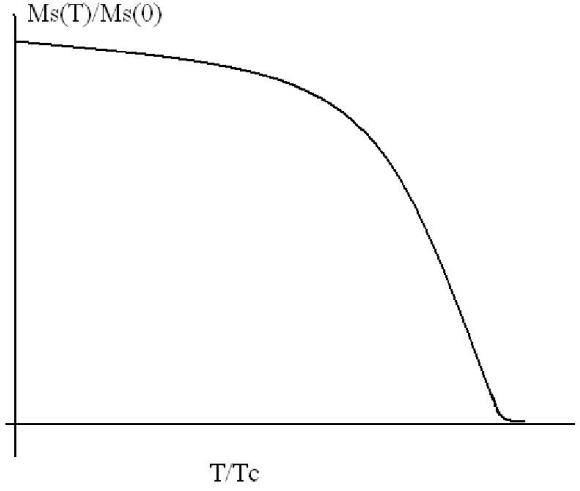

- Spontaneous magnetization, M_S of a ferromagnet as a function of reduced temperature T/T_C.
- Bloch's $T^{3/2}$ law holds only for $T/T_C << 1$.

Ferromagnetism

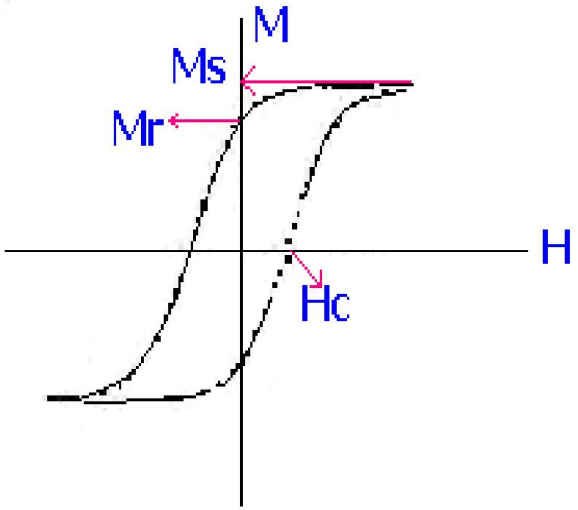

- **Hysteresis curve M(H)**

  M_S M_r H_C

- ***Permanent magnets:***

Ferrites: low cost, classical industrial needs,

H_C = 0.4 T.

NdFeB: miniaturization, actuators for read/ write heads, H_C = 1.5 T, very high energy product = 300 kJ/m^3.

AlNiCo & SmCo: Higher price/energy, used if irreplaceable.

Ferromagnetism

Ni Fe Cr Alloys

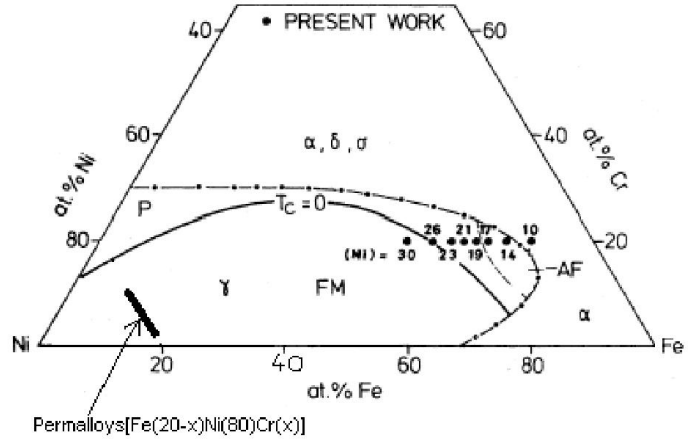

Soft magnetic materials

Used in channeling magnetic induction flux: Large $\mathbf{M_S}$ & initial permeability **μ**

Minimum energy loss (area of M-H loop).

Examples: Fe-Si alloys for transformers, FeB amorphous alloys for tiny transformer cores, Ferrites for high frequency & low power applications, YIG in microwave range, Permalloys in AMR & many multilayer devices.

Stainless steel (non-magnetic ???): Very interesting magnetic phases from competing FM/AFM interactions.

Collective-electron or band theory of ferromagnetism

The localized-moment theory breaks down in two aspects. The magnetic moment on each atom or ion should be the same in both the ferromagnetic and paramagnetic phases & its value should correspond to an integral number of μ_B. None are observed experimentally. Hence the need of a band theory or collective-electron theory. In Fe, Ni, and Co, the Fermi energy lies in a region of overlapping 3d and 4s bands as shown in Fig. 1. The **rigid-band model** assumes that the structures of the 3d and 4s bands do not change markedly across the 3d series and so any differences in electronic structure are caused entirely by changes in the Fermi energy (E_F). This is supported by detailed band structure calculations.

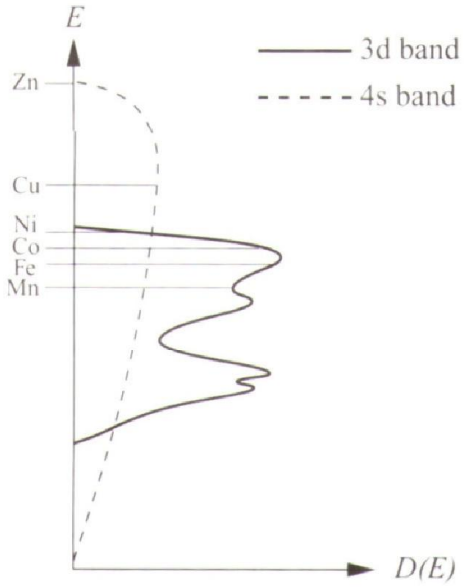

Fig. 1: Schematic 3d and 4s densities of states in transition metals. The positions of the Fermi levels (E_F) in Zn, Cu, Ni, Co, Fe, and Mn are shown.

Collective-electron or band theory of ferromagnetism

The exchange interaction shifts the energy of the 3d band for electrons with one spin direction relative to that with opposite spin. If E_F lies within the 3d band, then the displacement will lead to more electrons of the lower-energy spin direction and hence a spontaneous magnetic moment in the ground state (Fig. 2). The exchange splitting is negligible for the 4s electrons, but significant for 3d electrons.

- In Ni, the displacement is so strong that one 3d sub-band is filled with 5 electrons, and the other contains all 0.54 holes. So the saturation magnetization of Ni is $M_S = 0.54N\mu_B$, where N is the total number of Ni atoms. $\Rightarrow$ **the magnetic moments of the 3d metals are not integral number of μ_B!**
- In Cu, E_F lies above the 3d band. Since both the 3d sub-bands are filled, and the 4s band has no exchange-splitting, the numbers of up- and down-spin electrons are equal. Hence no magnetic moment.

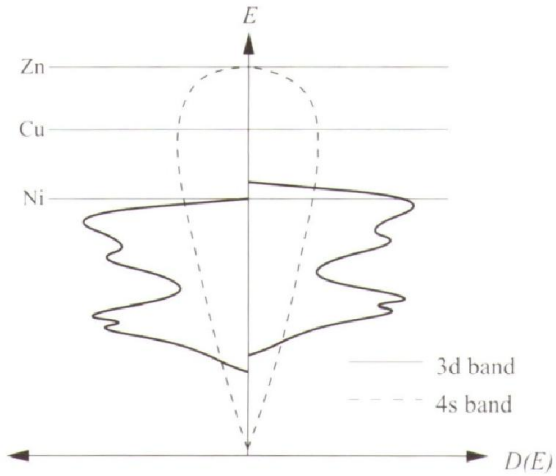

Fig. 2: Schematic 3d and 4s up- and down-spin densities of states in a transition metal with exchange interaction included.

- In Zn, both the 3d and 4s bands are filled and hence no magnetic moment.
- In lighter transition metals, Mn, Cr, etc., the exchange interaction is much weaker & ferromagnetism is not observed.

Band structure of 3d magnetic metals & Cu

$M_S = 2.2\ \mu_B$

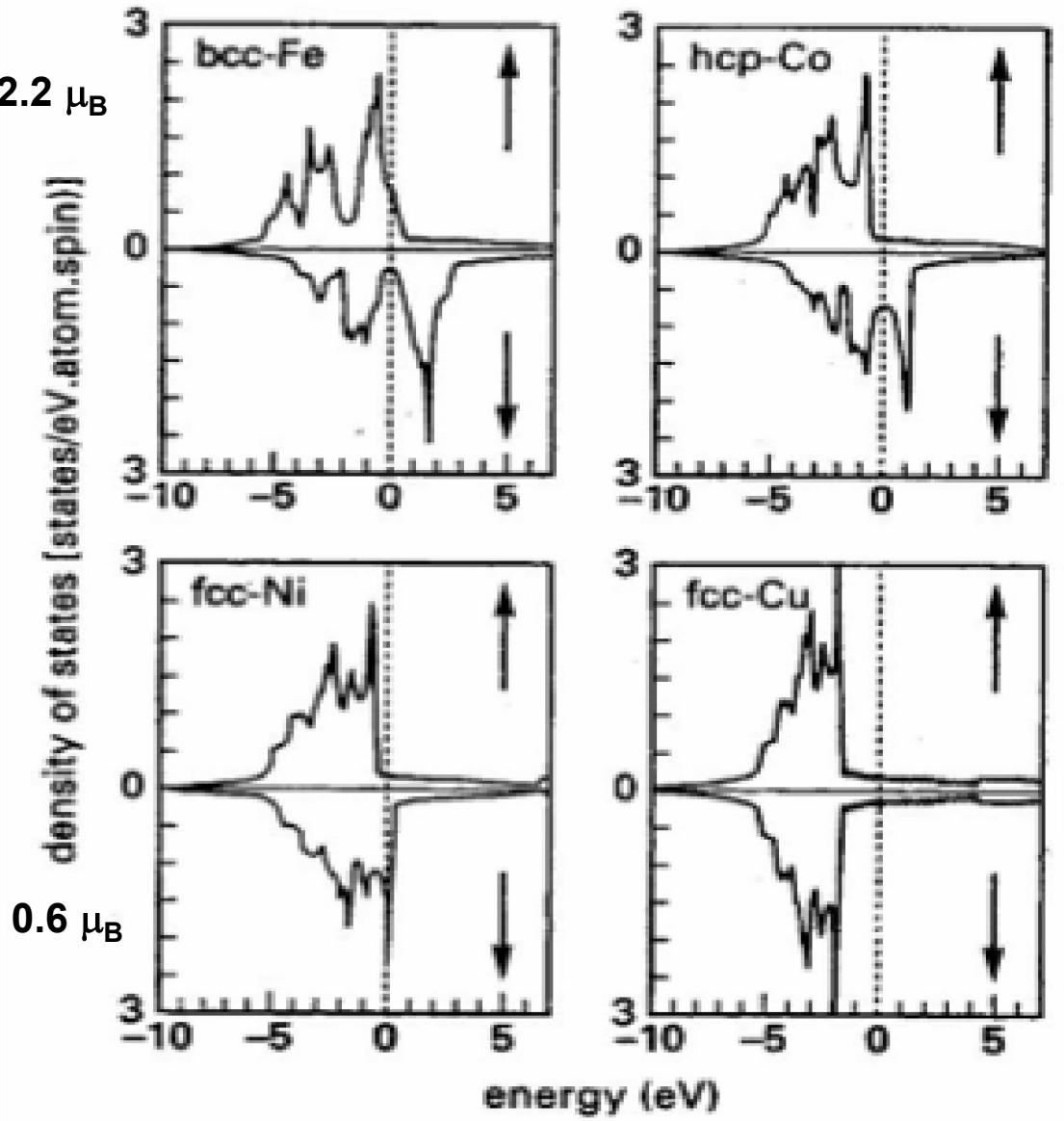

$M_S = 1.7\ \mu_B$

$M_S = 0.6\ \mu_B$

$M_S = 0.0\ \mu_B$

The Slater-Pauling curve(1930)

The collective-electron and rigid-band models are further supported by the well-known plot known as the Slater-Pauling curve. They calculated the saturation magnetization as a continuous function of the number of 3d and 4s valence electrons per atom across the 3d series. They used the rigid-band model, and obtained a linear increase in saturation magnetization from Cr to Fe, then a linear decrease, reaching zero magnetization at an electron density between Ni and Cu. Their calculated values agree well with those measured for Fe, Co, and Ni, as well as Fe-Co, Co-Ni, and Ni-Cu alloys. The alloys on the right-hand side are strong ferromagnets. The slope of the branch on the right is −1 when the charge difference of the constituent atoms is small, $Z \sim < 2$. The multiple branches (on left) with slope ≈ 1, as expected for rigid bands, are for alloys of late 3d elements with early 3d elements for which the 3d-states lie well above the Fermi level of the ferromagnetic host & we have to invoke Friedel's virtual bound states.

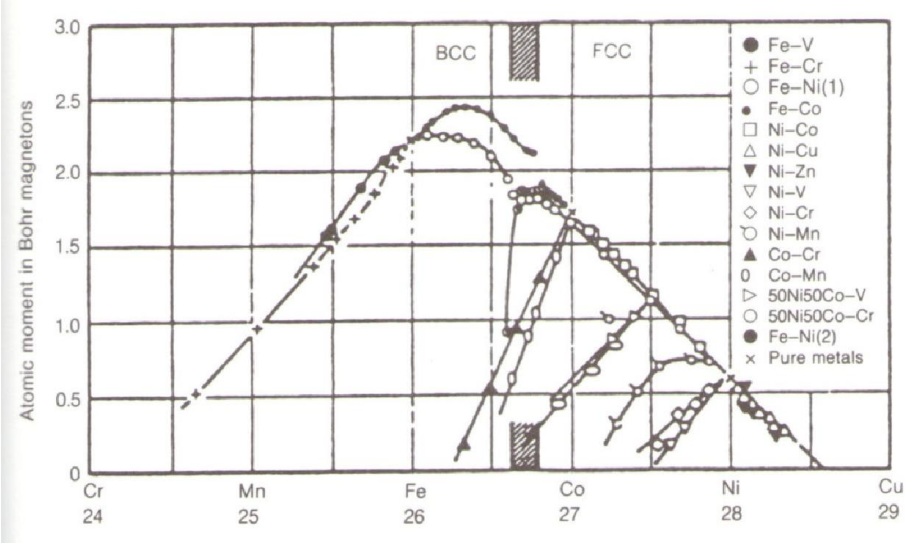

The average atomic moment is plotted against the number of valence ($3d + 4s$) electrons.

Stoner criterion

The Pauli susceptibility ($\mu_0 D(\varepsilon_F)\mu_B^2$) is approximately 10^{-5} for many metals, but it approaches 10^{-3} for 4d Pd . Narrower bands tend to have higher susceptibility, because the density of states $D(\varepsilon_F)$ scales as the inverse of the bandwidth. When $D(\varepsilon_F)$ is high enough, it becomes energetically favourable for the bands to split, and the metal becomes spontaneously ferromagnetic. Stoner applied Weiss's molecular field idea to the free-electron gas.

Assuming the linear variation of internal field with magnetization with a coefficient n_S : $H^i = n_S M + H$, the Pauli susceptibility in the internal field is $\chi_P = M/(n_S M + H)$. Hence, the response to the field H, $\chi = M/H = \chi_P/(1 - n_S \chi_P)$ is a susceptibility that diverges when $n_S \chi_P = 1$.

Stoner expressed this condition in terms of the local, $D(\varepsilon_F)$. Writing the exchange energy (in J m^{-3}) $-1/2\ \mu_0 H^i M = -1/2\ \mu_0 n_S M^2$ as $-(I/4)(n^\uparrow - n^\downarrow)^2/n$, where $M = (n^\uparrow - n^\downarrow)\mu_B$ and n is the number of atoms per unit volume, it follows that $n_S \chi_P = ID(\varepsilon_F)/2n$. The metal becomes spontaneously ferromagnetic when the susceptibility diverges spontaneously when $IN_{\uparrow,\downarrow}(\varepsilon_F) > 1$, where $N_{\uparrow,\downarrow}(\varepsilon) = D(\varepsilon)/2n$ is the density of states per atom for each spin state (See next slide for details).

This is the famous Stoner criterion. The Stoner exchange parameter I is roughly 1 eV for the 3d ferromagnets, and $n_S \sim 10^3$ for spontaneous band splitting. The exchange parameter has to be comparable to the width of the band for spontaneous splitting to be observed. Ferromagnetic metals have narrow bands and a peak in the density of states N(ε) at or near ε_F . Data show that only Fe, Co, and Ni meet the Stoner criterion. Pd comes very close.

Magnetic Anisotropies

The exchange interaction between spins in ferro- or ferrimagnetic materials is the main origin of spontaneous magnetization. This interaction is essentially isotropic, so that the spontaneous magnetization can point in any direction in the crystal without changing the internal energy, if no additional interaction exists. However, in actual materials, the spontaneous magnetization has an easy axis, or several easy axes, along which the magnetization prefers to lie. Rotation of magnetization away from the easy axis is possible only by applying an external magnetic field. This phenomenon is called magnetic anisotropy which is used to describe the dependence of the internal energy on the direction of spontaneous magnetization. An energy term of this kind is called **magnetocrystalline anisotropy energy**.

Magnetocrystalline or simply crystalline anisotropy energy is defined as the work required to make the magnetization lie along a certain direction compared to an easy direction. If the work is performed under isothermal condition, the crystalline anisotropy energy is nothing but the free energy, F. This is evident from the following derivation.

The free energy $F = U - TS$

so that

$$dF = dU - T\,dS - S\,dT = dU - dQ - S\,dT = -dW - S\,dT$$

where use has been made of the first law of thermodynamics, i.e., $dU = dQ - dW$. Thus, at constant temperature,

$$F = \int_0^F dF = \int -dW$$

Magnetic Anisotropies

Magnetocrystalline anisotropy

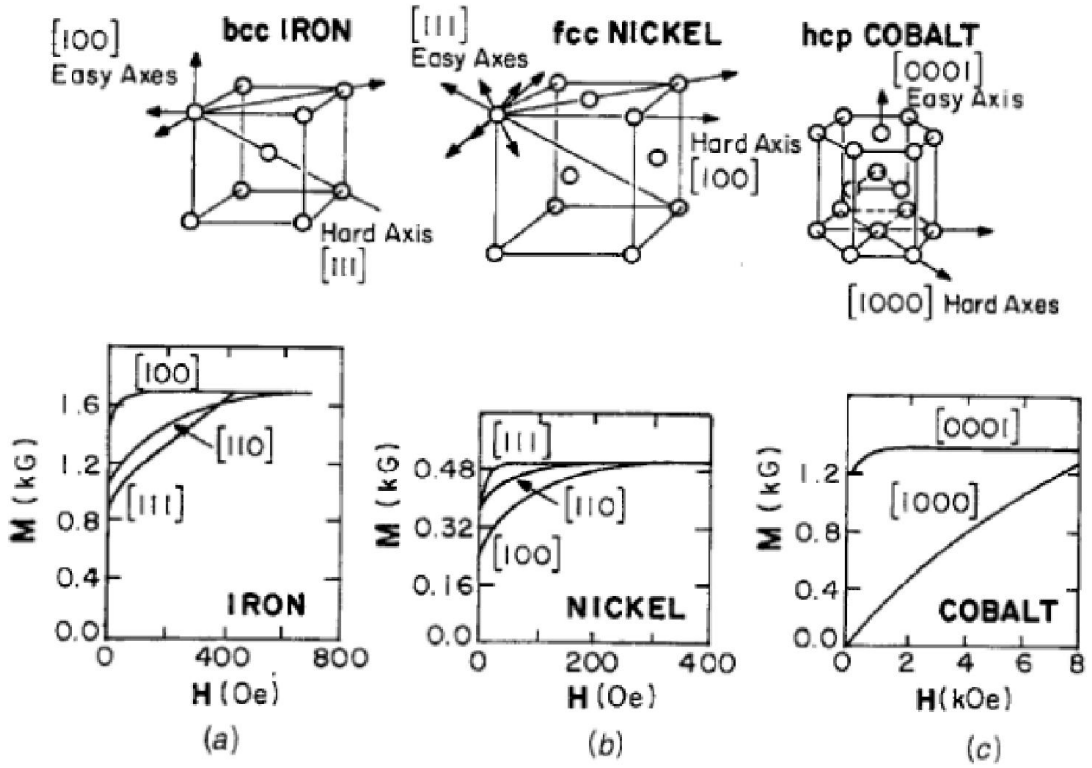

Crystal structure and magnetization curves taken along the easy and hard magnetization directions for (a) Fe, (b) Ni, and (c) Co.

Magnetic Anisotropies

For cubic crystals like iron and nickel, the anisotropy energy can be expressed in terms of the direction cosines (α_1, α_2, α_3) of the magnetization vector w. r. t. the three cube edges. There are many equivalent directions in which the anisotropy energy has the same value. Because of the high symmetry of the cubic crystal, the anisotropy energy can be expressed as a polynomial series in α_1, α_2, and α_3 . Those terms which include odd powers of α_I or cross-terms must vanish, because a change in sign of any of the α_i, should bring the magnetization vector to a direction which is equivalent to the original direction. The expression must also be invariant to the interchange of any two α_is. The first term, therefore, should have the form $\alpha_1^2 + \alpha_2^2 + \alpha_3^2$, which is always equal to 1 and hence no anisotropy can result. Next is the fourth-order term which can be reduced to the form $\sum_{i>j} \alpha_i^2 \alpha_j^2$ by the relationship

$$\alpha_1^4 + \alpha_2^4 + \alpha_3^4 = 1 - 2(\alpha_1^2\alpha_2^2 + \alpha_2^2\alpha_3^2 + \alpha_3^2\alpha_1^2).$$

Thus we have the expression

$$E_a = K_1(\alpha_1^2\alpha_2^2 + \alpha_2^2\alpha_3^2 + \alpha_3^2\alpha_1^2) + K_2\alpha_1^2\alpha_2^2\alpha_3^2$$

Soshin Chikazumi, Physics of Ferromagnetism, Oxford University Press (1996), Chapter 12.

Magnetic Anisotropies

K1 & K2 could be both positive & negative.

For iron at ~ 300 K: $K_1 = 4.8 \times 10^4$ J/m^3, $K_2 = \pm 0.5 \times 10^4$ J/m^3

For nickel at ~ 300 K: $K_1 = -0.45 \times 10^4$ J/m^3, $K_2 = 0.23 \times 10^4$ J/m^3

For (100) direction: $E_a = K_1$.

For (111) direction: $E_a = 3/2\ K_1 + 1/8\ K_2$.

For Fe: $E_a = 4.8 \times 10^4$ J/m^3 for (100) and $(7.14 - 7.26) \times 10^4$ J/m^3 for (111).

So (100) is the easy axis.

For Ni: $E_a = -0.45 \times 10^4$ J/m^3 for (100) and -0.65×10^4 J/m^3 for (111).

So (111) is the easy axis.

Hexagonal cobalt exhibits uniaxial anisotropy with the spontaneous magnetization, or easy axis, parallel to its c-axis of the at 300 K. As the magnetization rotates away from the c-axis, the anisotropy energy oscillates with θ, the angle between the c-axis and the magnetization vector. We can express this energy by expanding it in a power series in $\sin^2\theta$ as:

$$E_a = K_{u1} \sin^2 \theta + K_{u2} \sin^4 \theta \ .$$

For measuring magnetic anisotropy one uses techniques like torque magnetometer.

Magnetic Anisotropies

Origin of Magnetocrystalline Anisotropy: Van Vleck showed that magnetocrystalline anisotropy results when the spin-orbit interaction is considered as a perturbation to a system with isotropic Heisenberg exchange interactions. The second-order term in the perturbation expansion is:

$$J_{ex}\left(\frac{\lambda}{\Delta E}\right)^2\left[\boldsymbol{S}_i\cdot\boldsymbol{S}_j-\frac{3(\boldsymbol{S}_i\cdot\boldsymbol{r}_{ij})(\boldsymbol{S}_j\cdot\boldsymbol{r}_{ij})}{r_{ij}^2}\right]$$

where λ is the spin-orbit coupling constant and ΔE is the energy difference between the ground and excited energy states of the orbital levels. Except for the factor $J_{ex}(\lambda/\Delta E)^2$, this expression resembles that for the classical dipole-dipole interaction energy. Hence, this type of coupling is sometimes called pseudo-dipolar or anisotropic exchange. If the spins are treated as classical vectors, the pseudo-dipolar term averages out to zero in a crystal with cubic symmetry. This follows from the fact that the pseudo-dipolar coupling is proportional to $\left(1-3\,cos^2\theta_{ij}\right)$ and the average of $cos^2\theta_{ij}$ is 1/3. However, this is not the case when the spin orientations are quantized since the perturbation theory yields the energy correction to the second-order proportional to $J_{ex}(\lambda/\Delta E)^4$. Thus, when the anisotropy originates from the pseudo-dipolar interactions, perturbation theory predicts that $K_1 \approx J_{ex}\left(\frac{\lambda}{\Delta E}\right)^4$.

Ferromagnetic Domains

The stable domain structure minimizes the total energy consisting of magnetostatic, exchange, and anisotropy. Some typical domain structures and 180 & 90° walls (dashed lines) are:

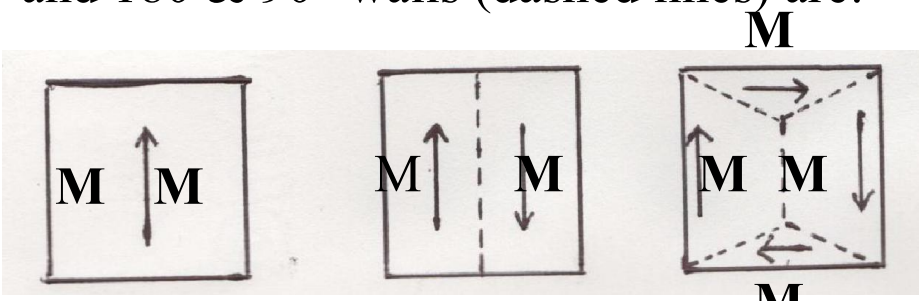

No wall 180° wall

→ 90° wall: Picture-frame domain

A domain wall (Bloch wall) in crystals is the transition region which separates adjacent domains magnetized in different directions. The spins don't change abruptly across a single atomic plane but rotate gradually over many planes. When a field is applied, the domain structure changes so as to increase **M** along the field. The spins inside the domains, being ↑ or ↓ to **H**, don't

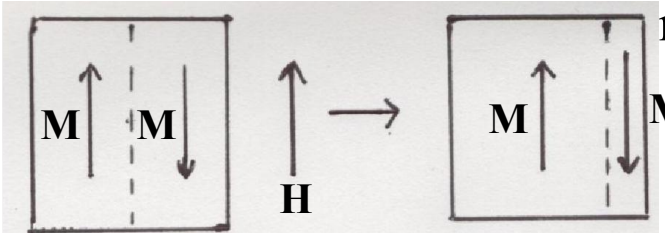

nce any torque. But those within the **H** and start to rotate towards H resulting in an increase in the volume of the domain ↑ to **H**.

This is called magnetization by "Domain wall displacement".

Ferromagnetic Domains

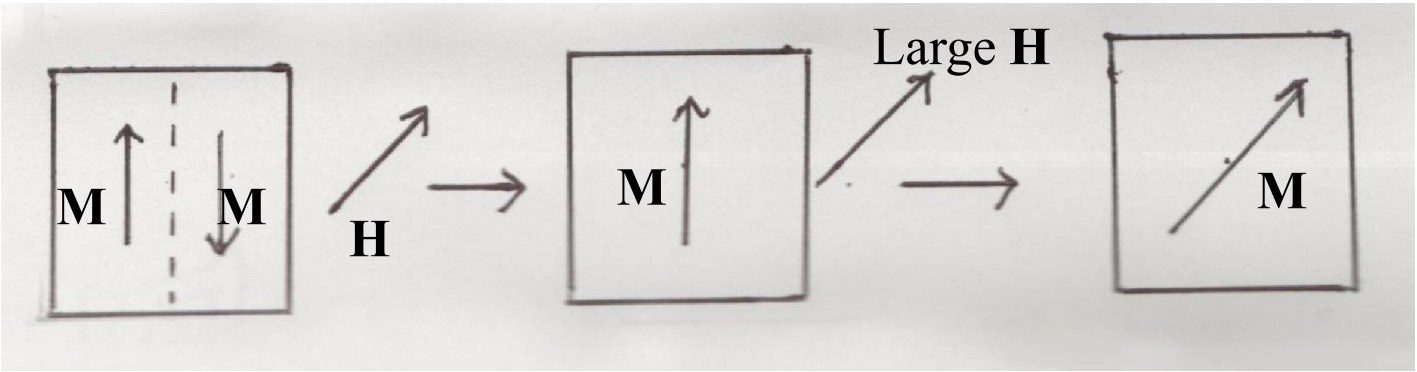

When **H** makes an angle with **M**, magnetization takes place initially by wall displacement at low fields increasing the volume of the favorably oriented domain at the cost of the unfavorably oriented ones. At higher fields **M** is rotated towards **H**.

Domain wall thickness: If the spin magnetic moments **S** of two adjacent atoms i and j make an angle ϕ_{ij}, the exchange energy is given by = $E_{ij} = -2JS^2 \cos \phi_{ij}$. For J > 0, the lowest energy state is where the two spins S are ∥. For $\phi_{ij} \ll 1$, $E_{ij} = JS^2 \phi_{ij}^2 + C$.

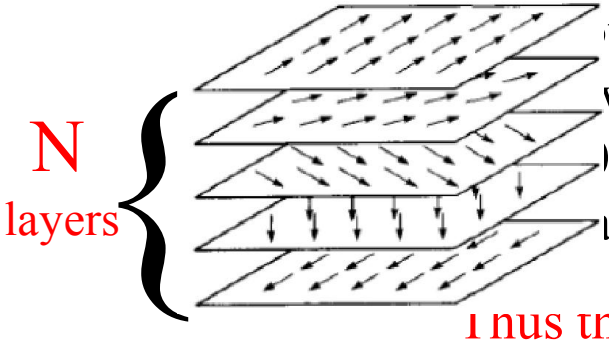

Consider 180° domain wall of N atomic layers; if tation is uniform, then, $\phi_{jj} = \pi/N$. For simple with lattice constant 'a', the no. of atoms/area 01) surface is $1/a^2$. The exchange energy stored in ll/area is $\gamma_{ex} = N E_{ij}/a^2 = JS^2\pi^2/a^2N$. (1)

Thus the exchange energy stored in the wall decreases with increasing no. of layers and hence the wall thickness.

Ferromagnetic Domains

On the other hand, the rotation of the spins in the wall out of the easy direction of magnetization causes an increase in the magnetocrystalline anisotropy energy. The anisotropy energy/area stored in this volume is

$$\gamma_a = K N a. \quad (2)$$

Domain wall thickness is determined by the balance between the exchange energy which tends to increase the thickness and the anisotropy energy which tends to diminish it.

$$\gamma_{total} = \gamma_{ex} + \gamma_a = JS^2\pi^2/a^2N + K N a. \quad (3)$$

Minimizing γ_{total} w. r. t. N: $\partial\gamma_{total}/\partial N = 0$ gives $N = (JS^2\pi^2/Ka^3)^{1/2}$.

Thus, the wall thickness $\delta = N a = (JS^2\pi^2/Ka)^{1/2}$. (4)

For iron $J = 2.16 \times 10^{-21}$ J, S = 1, $K = 4.2 \times 10^4$ J/m^3, $a = 2.86 \times 10^{-10}$ m and so the wall thickness $\delta = 4.2 \times 10^{-8}$ m $\approx$ 150 lattice constants & the total wall energy/area $\gamma_{total} = 2 (JS^2\pi^2K/a)^{1/2}$ (5)

$= 1.1 \times 10^{-3}$ J/m^2 = 1.1 ergs/cm^2.

Reference: Soshin Chikazumi, Physics of Ferromagnetism, Oxford University Press (1996), Chapters 15 to 17.

Ferromagnetic Domains

Domain thickness:

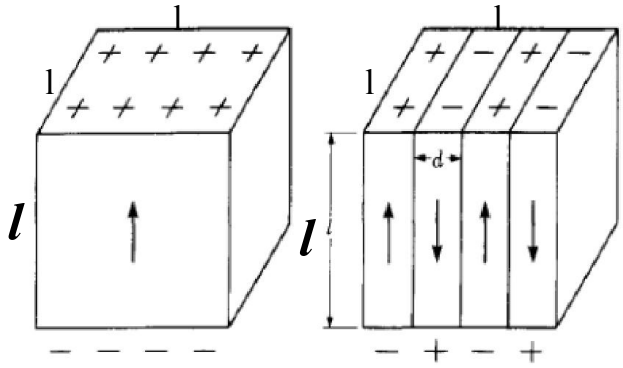

Fig. (a) Fig. (b)

Consider a ferromagnetic plate of length ***l***, unit surface area, and easy axis perpendicular to the plate. If there is a single domain [Fig. (a)] 'N' poles appear on the top surface & 'S' poles at the bottom producing a demagnetization field - M_S/μ_0.

The magnetostatic energy stored per unit area is

$$E_m = M_s^2\, l\, /2\mu_0. \qquad (6)$$

E_m gets lowered if the plate is divided into many laminated domains of thickness d [Fig. (b)]. Here also free poles exist on both top & bottom surfaces. If l » d, we can ignore the interaction between the free poles and find E_m increases with 'd' as $E_m = 1.08 \times 10^5\, M_s^2 d.$ (7)

On the other hand, domain wall energy decreases with the increase of 'd'. ***WHY ???*** Since γ_{total} [Eq. (5)] is the wall energy/area and ***l***/d is the total wall area (area of 1 domain x N domains = ***l*** x unit length x N = ***l*** N = ***l***/d since no. of domains is unit length/d), the wall energy area of the plate is

$$E_{wall} = \gamma_{total}\, l/d \qquad (8)$$

Ferromagnetic Domains

The equilibrium value of 'd' is determined by minimizing

$$E_{Total} = E_m + E_{wall} = 1.08 \times 10^5 M_s^2 d + \gamma_{total}\, l/d. \quad (9)$$

$$\partial E_{Total}/\partial d = 0 \text{ giving } d = 3 \times 10^{-3}(\gamma_{total} l)^{1/2}/M_S. \quad (10)$$

For iron with $\mu_0 M_S = 2.15$ tesla, assuming $l = 1$ cm

$$d = 5.6 \times 10^{-6} \text{ m} \approx 1/100 \text{ mm}.$$

Then, $E_{Total} = 6.56 \times 10^2 M_S (\gamma_{total} l)^{1/2} \approx 5.63 \text{ J/m}^2$.

If instead of many domains, there was a single domain (no wall energy),

$$E_{Total} = E_m = M_S^2 l/2\mu_0. \quad (6)$$

$$= 1.8 \times 10^4 \text{ J/m}^2.$$

Thus the energy is reduced by a factor of 3,000 by the generation of finely divided domains.

There are other more stable domain configurations among which the closure domain [See Fig. 90° wall: Picture- frame domain] is the most important one observed in cubic crystals, like say, 4% Si-Fe. There is no magnetostatic energy. Here the domain width is determined by the balance between the magnetoelastic and wall energies. For ferromagnets there is a spontaneous deformation along the easy axis called "magnetostriction".

Here E_{Total} is 300,000 times smaller than the one without domains.

Magnetism

Paramagnetism

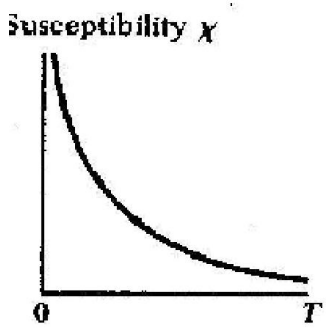

$$\chi = \frac{C}{T}$$

Curie law

Ferromagnetism

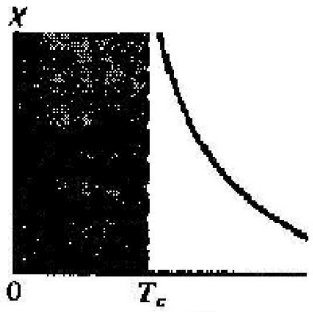

$$\chi = \frac{C}{T - T_c}$$

Curie-Weiss law
$(T > T_c)$

Antiferromagnetism

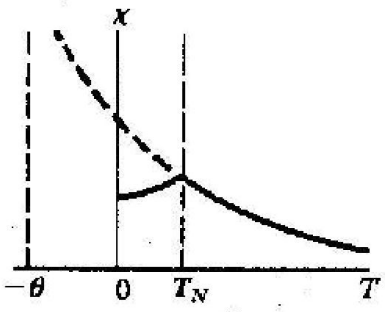

$$\chi = \frac{C}{T + \theta}$$

$(T > T_N)$

FERRIMAGNET

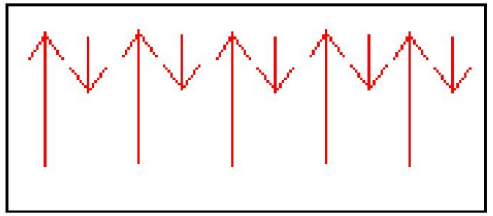

FERROMAGNET

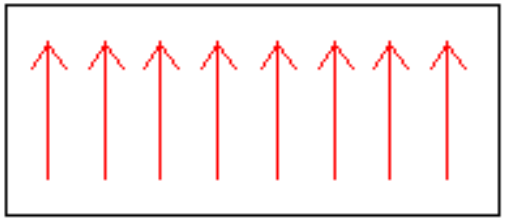

ANTIFERROMAGNET

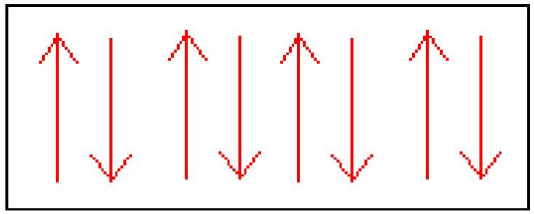

Indirect exchange

There are a number of indirect exchange interaction mechanisms which, within the framework of second-order perturbation theory, lead to an effective Hamiltonian of the Heisenberg form. The different types of indirect coupling mechanisms are as follows:

Kondo effect (a few ppm level of magnetic ions in a sea of electrons of a noble metal host like CuMn, AuFe, etc.) is the dilute-limit indirect exchange interaction between 3d moments mediated by conduction electrons. The latter are magnetized in the vicinity of the magnetic ion. This magnetization causes an indirect exchange interaction between the two ions because a second ion perceives the magnetization induced by the first. This gives rise to the resistivity minima at low temperatures. Kondo had shown that the anomalously large scattering probability by magnetic ions is a consequence of the dynamic nature of the scattering by the exchange coupling and sharpness of the Fermi surface. The spin-dependent contribution to the resistivity $\boldsymbol{\rho_{mag} \sim J \ln T}$. If the exchange energy J is negative the spin resistivity increases as T is lowered. Adding to $\rho_{mag} = - c \rho_1 \ln T$ the residual resistivity and the phonon term $\boldsymbol{c\rho_0 + aT^5}$ and minimizing ρ w. r. t T we get Kondo temperature $\boldsymbol{T_{min} = (c\rho_1/5a)^{1/5}}$ in agreement with experiments.

RKKY interactions

Then comes the **RKKY** (Rudermann-Kittel-Kasuya-Yoshida) indirect exchange interaction in a metallic magnet such as Gd, dilute Cu-Mn alloys, etc. which is mediated by quasi-free conduction electrons. In most rare-earth compounds, their s and d electrons are delocalized and the ions are trivalent. The 4f electrons are very strongly bound and their orbitals are highly compact. Their spatial extension is far less than the interatomic spacing and so there cannot be any direct interaction of the 4f electrons of different atoms. Rather, it is the conduction electrons which couple the magnetic moments. This interaction can be written in terms of the 4f spins localized on the ion, $\mathbf{S}_i$ and of the spins of the conduction electrons, $\sigma(\mathbf{r})$:

$$E = -\sum_{R_i,\, r} J\,(\mathbf{R}_i - \mathbf{r})\, \mathbf{S}_i \cdot \sigma(\mathbf{r}).$$

This interaction is positive and highly localized of the form $J\,(\mathbf{R}_i - \mathbf{r}) = J\,\delta\,(\mathbf{R}_i - \mathbf{r})$ [intra-atomic exchange], $J \sim 10^{-1}$ to 10^{-2} eV. A conduction electron sees a rare earth site i through a **field** created by the spin of the rare earth $\mathbf{h}_i = J\mathbf{S}_i/g\mu_B\mu_0$. This field polarizes the conduction electrons and this polarization propagates through the lattice, creating at any other point j a magnetization of the conduction electrons. This magnetization of the conduction electrons, associated with the local field $\mathbf{h}_j$ at another site j, is described by the generalized susceptibility

RKKY interactions

χ_{ij} defined by $\mathbf{m_i = \chi_{ij}\, h_j = \chi_{ij}\, JS_j/g\mu_B\mu_0}$.

This amounts to an indirect interaction between the spins/magnetic moments on the two sites i and j. The interaction energy can be written as

$$\mathbf{E_{ij} = - Jm_i.S_i/g\mu_B = - J^2\chi_{ij}S_i.S_j/\mu_0(g\mu_B)^2.}$$

Clearly, this exchange interaction between spins is due to the polarization of the conduction electrons by localized spins. The sign of the interaction depends on the structure of the conduction band via χ_{ij}. For free electrons it acts at long distance and for $k_FR_{ij} >> 1$, $\mathbf{\chi_{ij} \sim -[2\, k_FR_{ij}cos(2\, k_FR_{ij}) - sin(2\, k_FR_{ij})]/(2\, k_FR_{ij})^4}$,

where k_F is the wave-vector at the Fermi level.

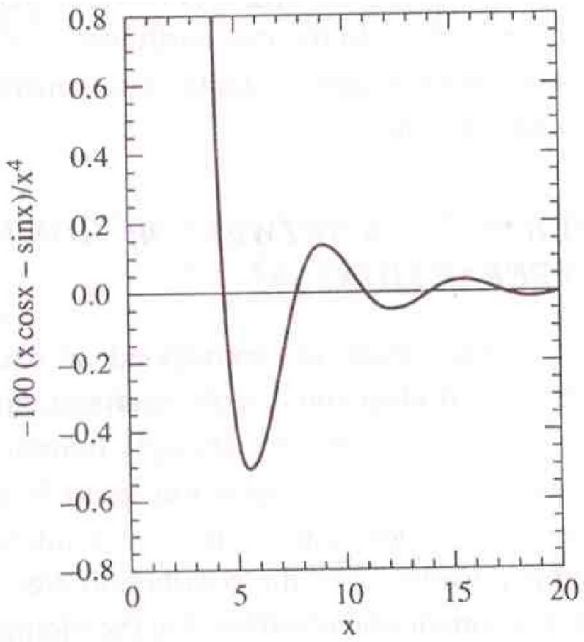

Thus the exchange oscillates as a function of the distance between spins, R_{ij} as shown. k_F determines the wavelength of this oscillation. RKKY interaction gives rise to ferromagnetism when k_F is small (nearly empty band) or antiferromagnetism when $k_F \sim \pi/a$ (half-filled band). We shall see in **GMR** that the same long-range interaction is generally the origin of coupling between magnetic layers which can be varied by changing the thickness of the non-magnetic layer. Also in **spin-glasses**.

Super-exchange

In magnetic insulators RKKY interaction cannot operate because of no free electrons. An indirect exchange mechanism that is relevant to magnetic insulators is the **super-exchange** as in MnO, NiO, MnF_2, CoF_2 systems. The partially filled magnetic d-shells of Mn^{2+}, Mn^{3+}, Ni^{2+}. Ni^{3+}, Fe and Co ions are separated by ~ 4 A and so have hardly any nearest neighbours and hence no direct exchange. Instead, the magnetic ion spins couple indirectly via the intervening non-magnetic (diamagnetic) oxygen or fluorine ions. This invariably leads to a long-range antiferromagnetic ordering of spins on the 3d transition metal cations.

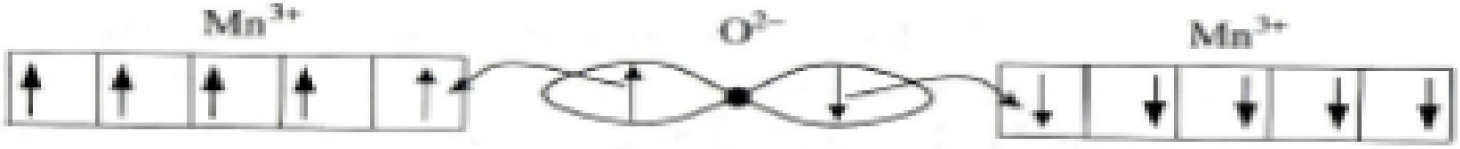

Due to a strong overlap of the 3d-wavefunctions of cations with 2p-wavefunctions of oxygen anions, electron hopping is possible. Mn^{3+} is $3d^4$. So, by Hund's rule we put their spins ‖ along ↑, say. Now it (Mn^{3+} on the left) can take only ↑ spin electron from O^{2-}. The second O^{2-} electron with spin ↓ can go to Mn^{3+} on the right whose all 4 spins MUST be ↓ to satisfy Hund's rule.

Hence, super-exchange favors antiferromagnetism.

Spin glass

- Figures below show formation of a spin glass which is an alloy of
  - Noble Metals(Cu, Ag, Au) – provides s conduction electrons.
  - 3d-Transition Metals(Cr, Mn, Fe, etc.) - provides localized d electrons.

KONDO REGIME

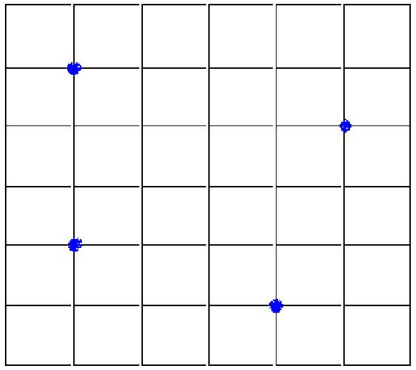

- **Kondo effect gives rise to resistivity minima**
  - **$\rho \sim J \ln T \sim - \ln T$ if $J < 0$ in case of AF**

SPIN GLASS

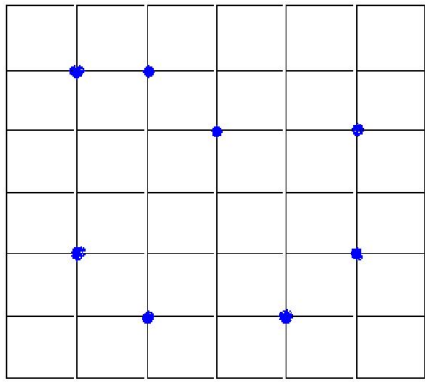

- **s-d interaction gives RKKY interaction ~ $\cos(2k_f r)/(2k_f r)^3$**

MICTOMAGNET

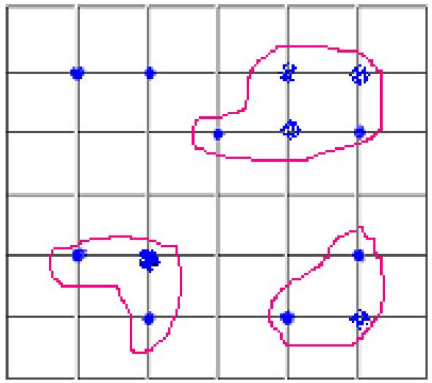

- **d-d overlap and s-d interaction**
- **CuMn (LRAF)**
- **AuFe (LRF)**

Spin glass

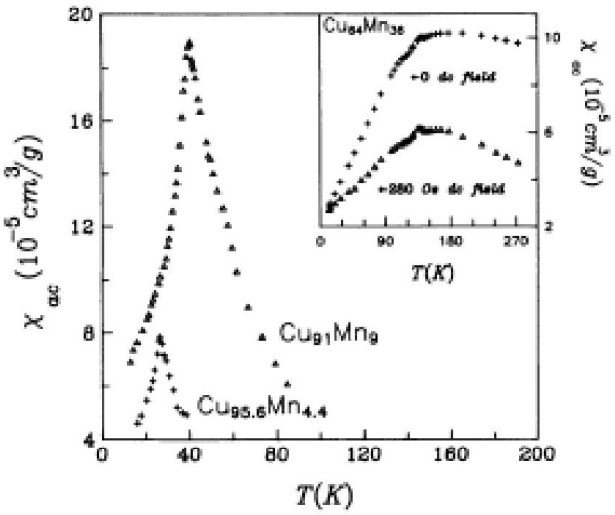

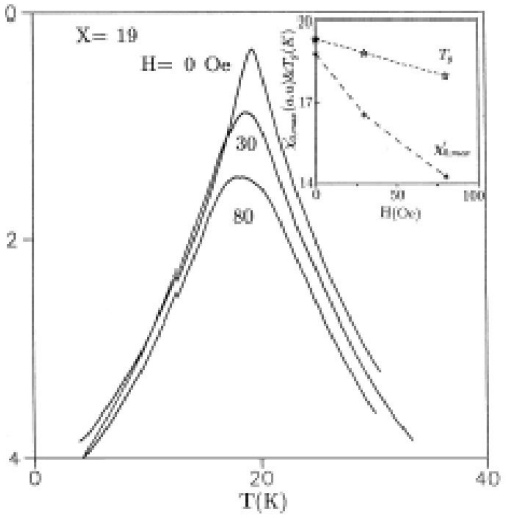

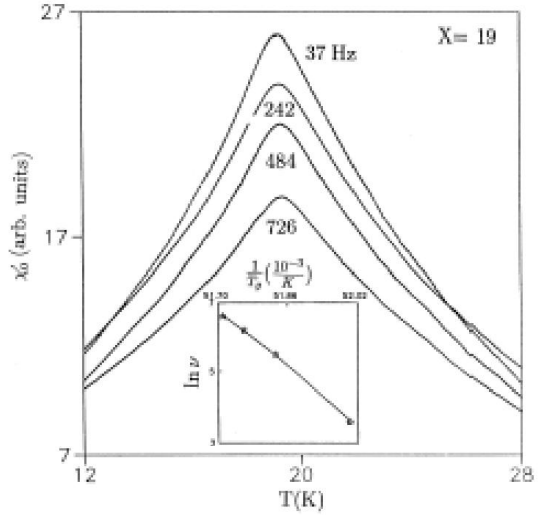

- *Temperature dependence of χ at several compositions.*

Temperature dependence of χ with variation of dc magnetic field.

- *Temperature dependence of χ with variation of frequency.*

EXPERIMENTS ON SPIN GLASS

Sharp anomaly	Smeared behavior
1) *Magnetic susceptibility*	1) *Specific Heat*
2) *Remanence & time dependence*	2) *Resistivity*
3) *Mossbauer effect*	3) *Thermal power*
4) *Muon spin rotation*	4) *Neutron scattering*
5) *Anomalous Hall effect*	5) *Ultrasonic velocity*

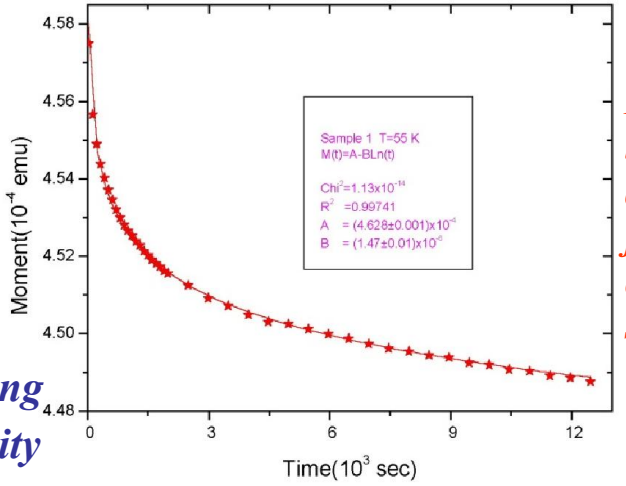

Logarithmic time decay of a field-cooled spin glass.

Spin glass

$t = 0$

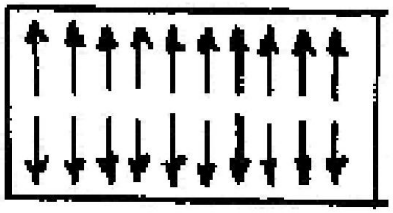

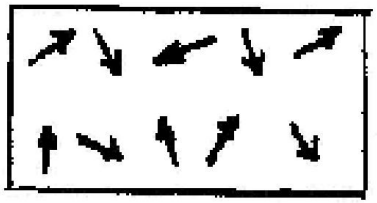

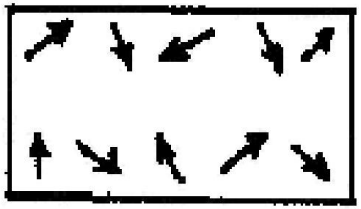

<m>=0 at T=0

$t = \infty$

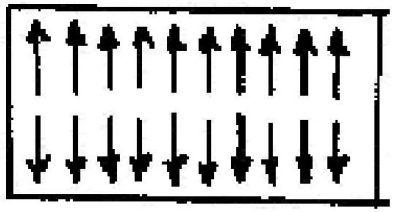

Antiferromanet
T< Tn
<m> ≠ 0

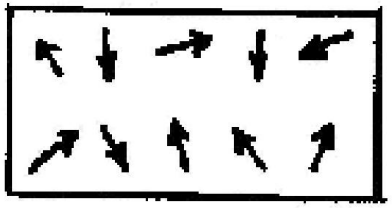

Paramagnet
T>>Tn/Tc
<m>=0

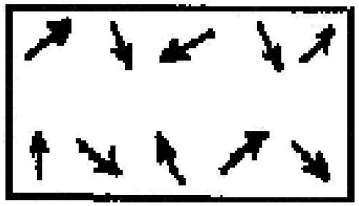

Spin-glass
T< Tsg ; <m> = 0
<q> ≠ 0

- **To distinguish between an antiferromagnet, a paramagnet and a spin glass.**

$$Q = \lim_{|t_1 - t_2| \to \infty} \overline{\langle S_i(t_1) S_i(t_2) \rangle}$$

Neutron scattering gives m = 0 but Q ≠ 0 for $T < T_g$.

R & D in Magnetic Materials after 1973

- The research on magnetism till late 20th century focused on its basic understanding and also on applications as soft and hard magnetic materials both in crystalline and amorphous forms.

- In 1980's it was observed that surface and interface properties deviate considerably from those of the bulk. With the advent of novel techniques like
  - e-beam evaporation
  - Ion-beam sputtering
  - Magnetron sputtering
  - Molecular beam epitaxy (MBE)

  excellent magnetic thin films could be prepared with tailor-made properties which can not be obtained from bulk materials alone.

  Magnetic recording industry was also going for miniaturization and thus the magnetic thin film technology fitted their requirement.

R & D in Magnetic Materials after 1973

- Then came, for the first time, the industrial application of electronic properties which depend on the spin of the electrons giving rise to the so-called Giant Magnetoresistance(GMR), discovered in 1986.

- Since early 80's the Anisotropic Magnetoresistance effect (AMR) has been used in a variety of applications, especially in read heads in magnetic tapes and later on in hard-disk systems, gradually replacing the older inductive thin film heads. GMR recording heads are already in the market for hard disk drives and offer a stiff competition to those using AMR effects.

So, what is Magnetoresistance ???

Magnetoresistance

I. Ordinary or normal magnetoresistance (OMR)

- Due to the Lorentz force acting on the electron trajectories in a magnetic field. MR ~ B^2 at low fields. MR is significant only at low temperatures for pure materials at high filds.

II. Anisotropic magnetoresistance (AMR) in a ferromagnet

- In low field LMR is positive and TMR is negative.
- Negative MR after saturation due to quenching of spin-waves by magnetic field.
- FAR is an inherent property of FM materials originating from spin-orbit interaction of conduction electrons with localized spins.
- FAR(ferromagnetic anisotropy of resistivity) $= (\Delta\rho_{//s} - \Delta\rho_{\perp s})/\rho_{//s}$

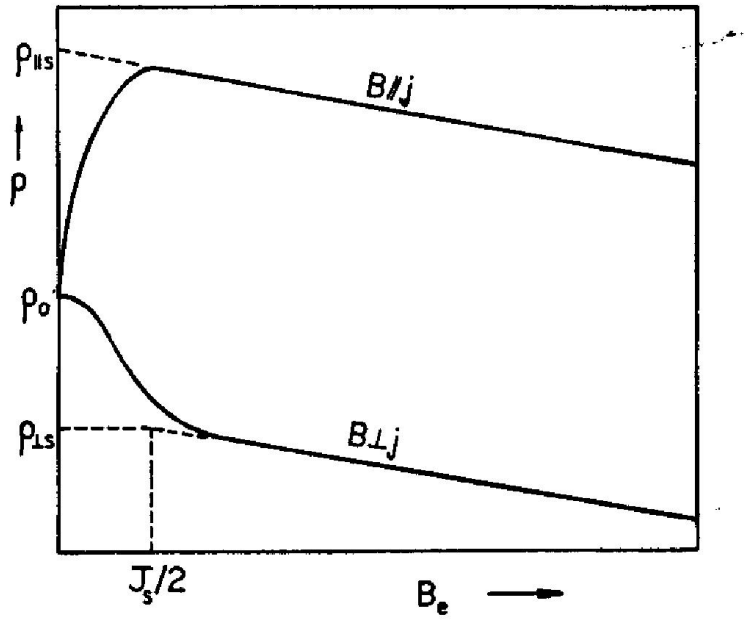

Magnetoresistance

III. Giant Magnetoresistance (GMR)

Fe-Cr is a lattice matched pair : Exchange coupling of ferromagnetic Fe layers through Cr spacers gives rise to a negative giant magnetoresistance (GMR) with the application of a magnetic field.

- RKKY interaction ~ $\cos(2k_f r)/(2k_f r)^3$.
- Established by experiments on light scattering by spin waves.

[P. Grünberg et al., Phys. Rev. Lett. 57, 2442(1986).]

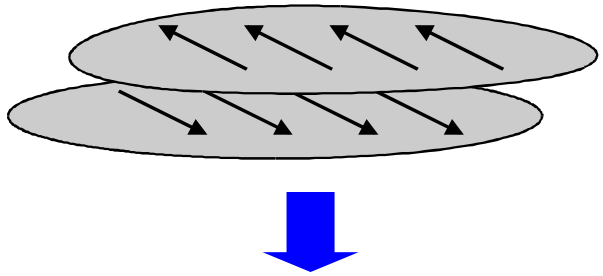

At low fields the interlayer antiferromgnetic coupling causes the spins in adjacent layers to be antiparallel and the resistance is high

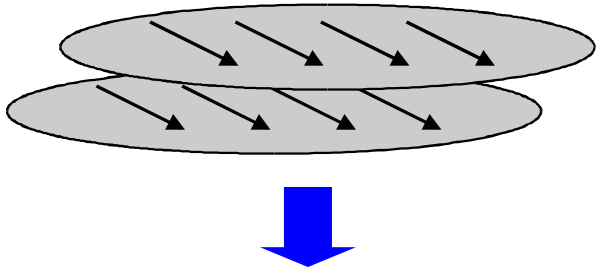

At high fields the spins align with the field (saturating at H_{sat}) and the resistance is reduced.

Magnetoresistance is negative!

Giant Magnetoresistance (GMR)

Magnetoresistance is defined by

$$MR = \frac{\rho(H,T)-\rho(0,T)}{\rho(0,T)}\times 100\% \quad . \qquad (1)$$

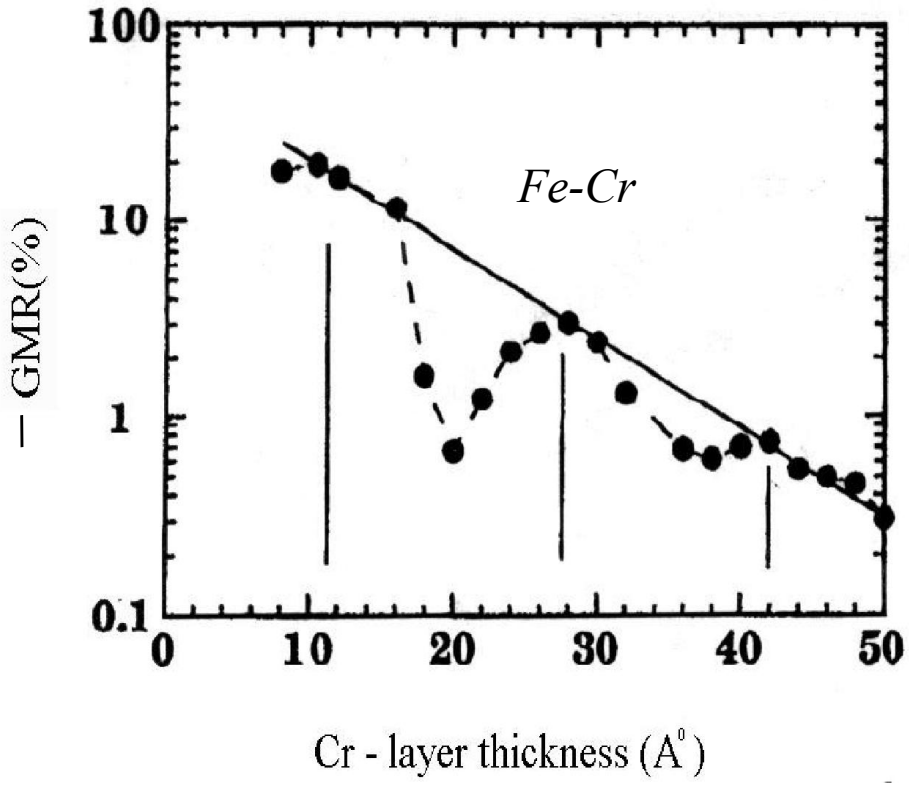

Giant Magnetoresistance (GMR)

Calculation of GMR (Spin-dependent scattering)

Bulk scattering

Assuming MFP > Cr spacer thickness. Spin-dependent scattering in ferromagnetic metals $\Rightarrow$ 2 current conduction model of Fert & Campbell.

[A. Fert and I. A. Campbell, J. Phys. F : Metal Phys., 6, 849(1976).]

In Fe (weak ferromagnet) majority band has a much lower conductivity as seen from $\sigma = ne\mu$ and its band structure.

[P. B. Visscher and Hui Zhang, Phys. Rev. B 48,

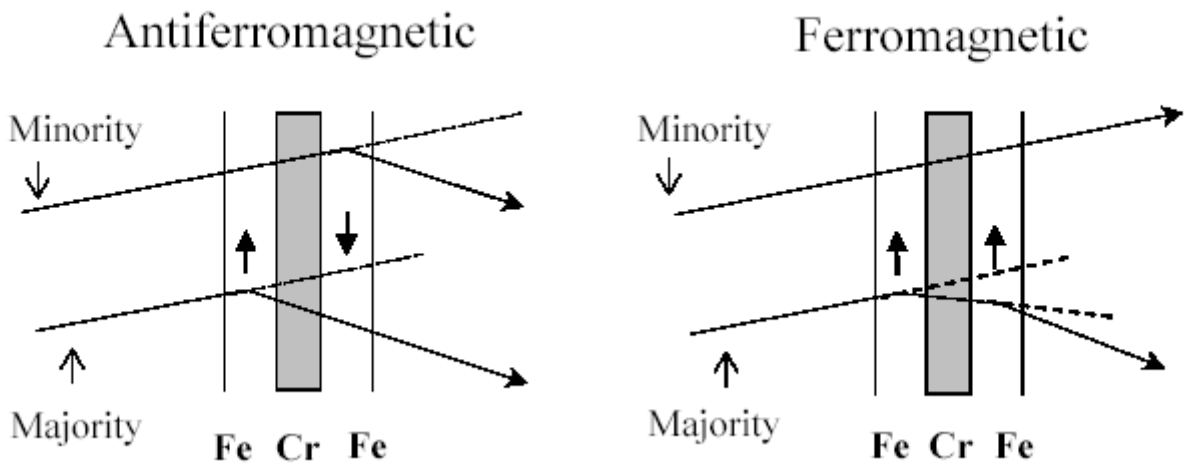

Giant Magnetoresistance (GMR)

Using the above picture one can show that

$$\mathrm{GMR} = -\left(\frac{\rho\downarrow/\rho\uparrow - 1}{\rho\downarrow/\rho\uparrow + 1}\right)^2,$$

where $\rho\downarrow$ and $\rho\uparrow$ are the resistivities of minority and majority band, respectively. It is the imbalance between $\rho\downarrow$ and $\rho\uparrow$ which produces GMR.

Interface scattering , alloying of Fe and Cr at the interface, etc. are also spin-dependent and contribute to GMR , so does the spin-flip scattering at high temperatures.

Magnetic Multilayers and Giant Magnetoresistance, Ed. by Uwe Hartmann, Springer Series in Surface Sciences, Vol. 37, Berlin (1999).

Giant Magnetoresistance (GMR)

Interface scattering

Local spin density approximation to density functional theory, treating the disordered atomic planes by KKR-CPA, was used by Butler et al. to calculate the electronic structure, magnetic moments, scattering rate and electrical conductivity in many GMR systems.

[W. H. Butler et al, J. Magn. Magn. Mater. 151, 354-362(1995)]

Calculated majority and minority valence electrons per atom for a trilayer system of 10 atomic layers of Cr embedded in Fe. Note the matching at the minority channel.

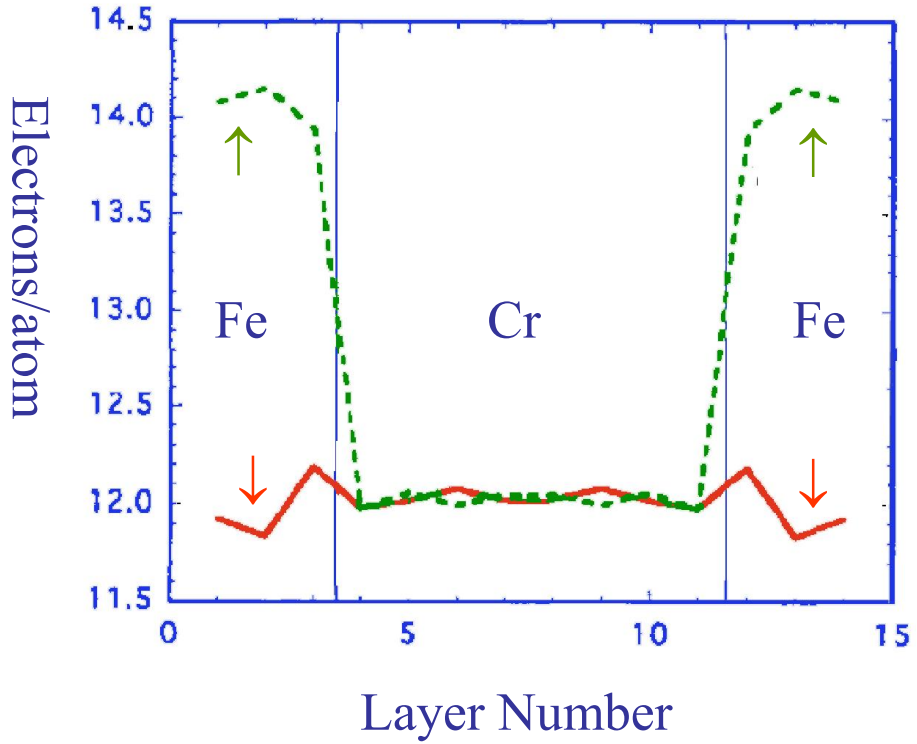

Giant Magnetoresistance (GMR)

So minority spin electrons at the Fermi level would see hardly any difference between the atomic potentials of Fe and Cr & experience weak reflections from interfaces and weak impurity scattering at interdiffused Fe-Cr zone. Significant contribution to GMR thus comes from the spin-dependent potential matching.

Calculations also show that the density of states at the matched spin channel is low.

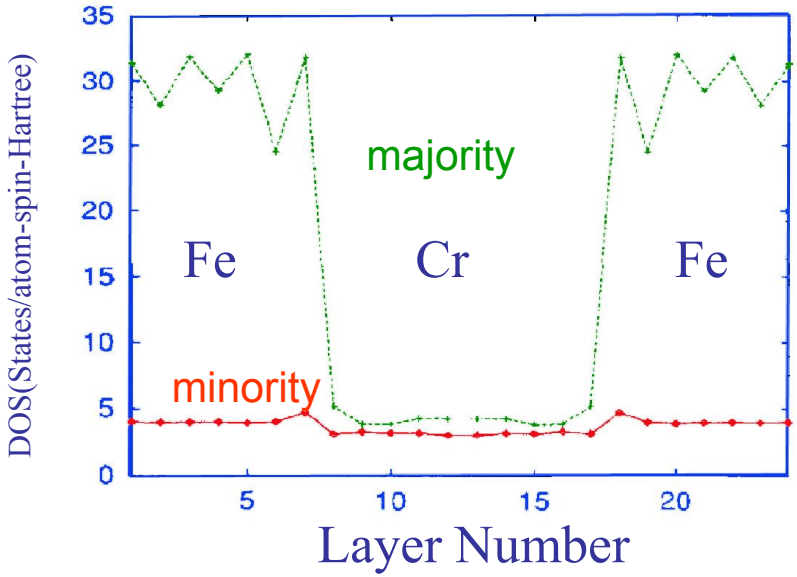

DOS in Fe-Cr trilayer shows large values for the majority carriers which show no band matching.

Giant Magnetoresistance (GMR)

Impurity scattering relaxation time τ_s^i of electrons with spin s goes as

$$\left\langle \frac{1}{\tau_s^i} \right\rangle \sim N_s(E_F) \left\langle | \Delta V_s |^2 \right\rangle,$$

where $N_s(E_F)$ is the DOS at E_F and ΔV_s is the difference in potential between the host and the impurity. This is valid only for $\Delta V_s \rightarrow 0$. $\Delta V_s \sim \sin^2\eta_l$; η_l = phase shifts of the host and the impurity potentials. Calculations of Butler et al. show that although s & p (l = 0 & 1) phase shifts are almost the same for the two channels they are very different for l = 2 (d↓ than d↑). So in the case of Cu-Co, the resistivity is much larger for the minority band due to its higher DOS as well as $\sin^2\eta_l$.

Electron-phonon scattering, dominant at higher temperatures, also has a similar dependence on DOS resulting in a higher resistivity for the minority band.

Giant Magnetoresistance (GMR)

Sample structure (GMR)

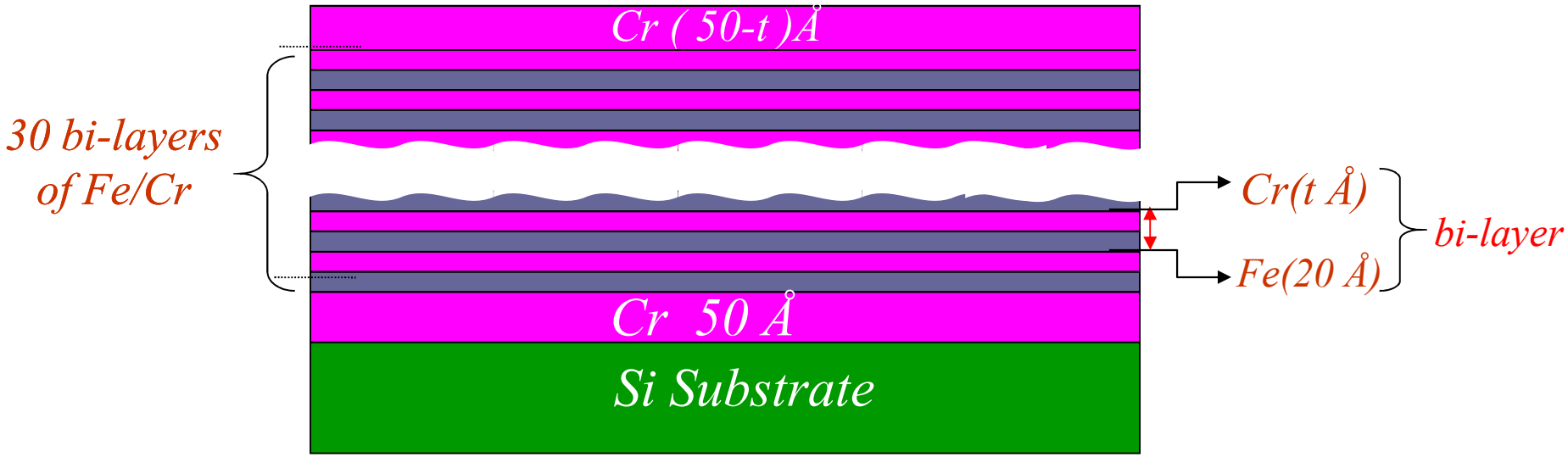

Sample details

- Si/Cr(50Å)/[Fe(20Å)/Cr(tÅ)]×30/Cr((50-t)Å)

  Varying Cr thickness t = 6, 8, 10, 12, and 14 Å
- Fe/Cr multilayers prepared by ion-beam sputtering technique.
- Ar and Xe ions were used.
- Beam current 20 mA /30 mA and energy 900eV/1100eV.

Giant Magnetoresistance (GMR)

GMR data in Fe-Cr multilayers

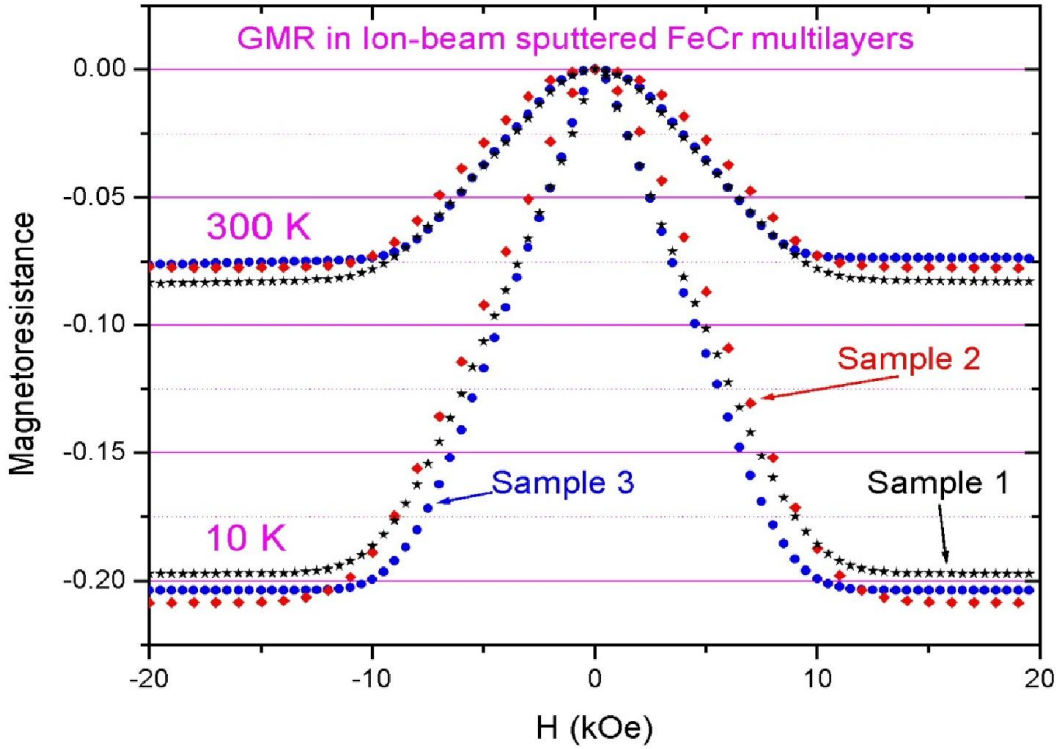

GMR vs. H for 3 samples.

- Negative GMR of 21% at 10K and 8% at 300K with $H_{sat} \approx$ 13 kOe.
- Hardly any hysteresis $\Rightarrow$ strong AF coupling.

GMR (H,T) ➔ A. K. Majumdar, A. F. Hebard, A. Singh, and D. Temple, Phys. Rev. B65,054408(2002).
Hall Effect (H,T) ➔ P. Khatua, A. K. Majumdar, D. Temple, and C. Pace, Phys. Rev. B73, March (2006).

Giant Magnetoresistance (GMR)

Application of GMR

1973: Rare earth – transition metal film in magneto-optic recording.
1979: Thin film technology for heads in hard disks (both read and write processes) (IBM).
1991: AMR effect using permalloy films for sensors in HDD by IBM.
1997: GMR sensors in HDD by IBM.

- Robotics and automotive sensors (e.g. in car).
- Pressure sensors(GMR in conjunction with magnetostrictive materials).
- Sensitive detection of magnetic field.
- Magnetic recording and detection of landmines.

Currently both GMR and TMR are used for application in sensors and MRAMs.

Comparison between AMR / GMR effect: In contrast to AMR, GMR is isotropic & is more robust than AMR.

GMR & Exchange-biased Spin-valve structure

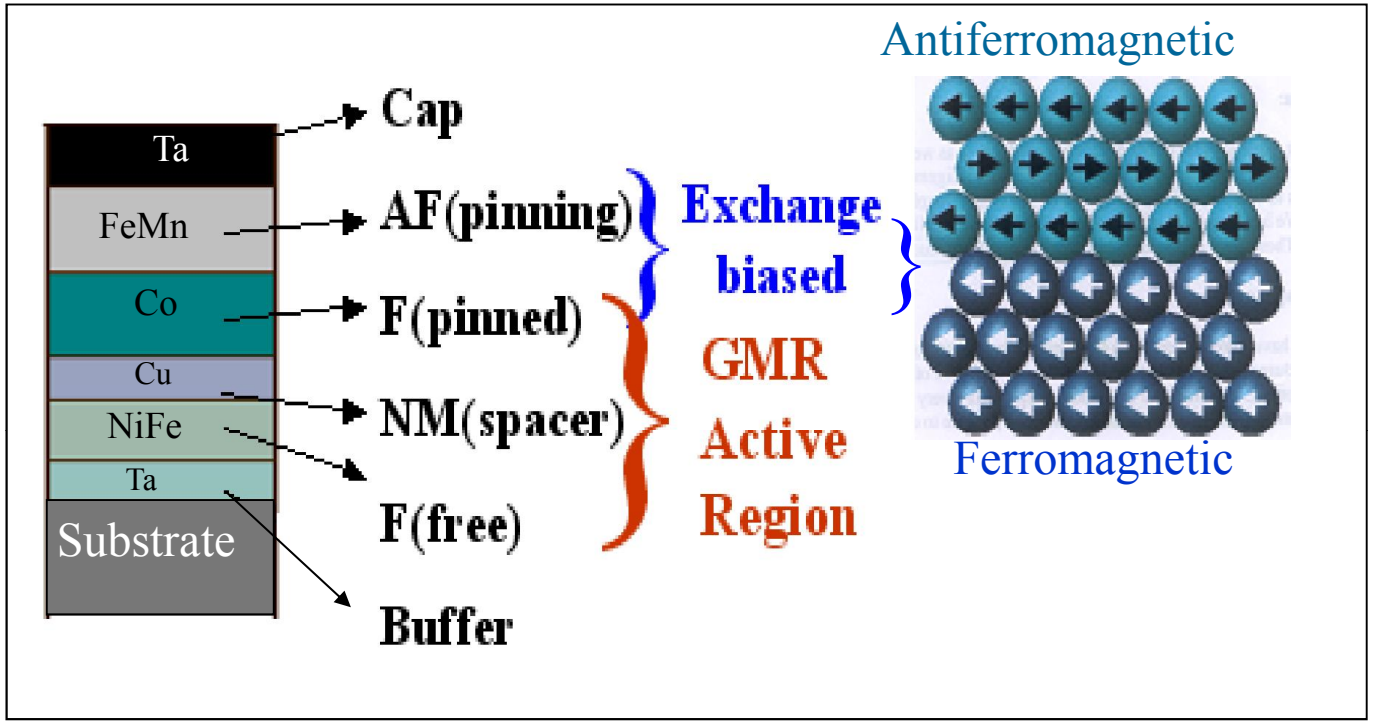

- FeMn providing local magnetic field to Co layer, and NiFe is magnetically soft.
- GMR > 20 %.
- Read heads for HDD detect fields ~ 10 Oe.

Tunnel Magnetoresistance (TMR)

Discovery of GMR effect in Fe/Cr supperlattice in 1988 and giant tunnel magnetoresistance (TMR) effect at room temperature (RT) in 1995 opened up a new field of science and technology called spintronics. The investigation provides better understanding on the physics of spin-dependent transport in heterogeneous systems. Perhaps more significantly, such studies have contributed to new generations of magnetic devices for information storage and magnetic sensors.

A magnetic tunnel junction (MTJ), which consists of a thin insulating layer (a tunnel barrier) sandwiched between two ferromagnetic electrode layers, exhibits TMR due to spin-dependent electron tunneling. MTJs with an amorphous aluminium oxide (Al–O) tunnel barrier have shown magnetoresistance (MR) ratios up to about 70 % at RT and are currently used in magnetoresistive random access memory (MRAM) and the read heads of hard disk drives. In 2004 MR ratios of about 200 % were obtained in MTJs with a single-crystal MgO(001) barrier or a textured MgO(001) barrier. Later CoFeB/MgO/CoFeB MTJs were also developed having MR ratios up to 500 % at RT.

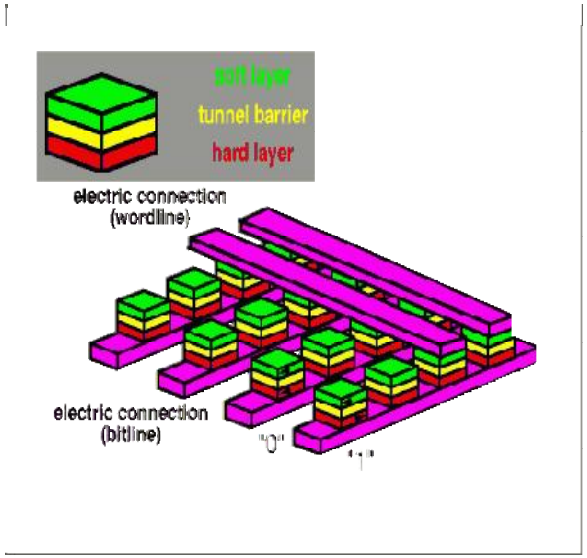

Tunnel Magnetoresistance (TMR)

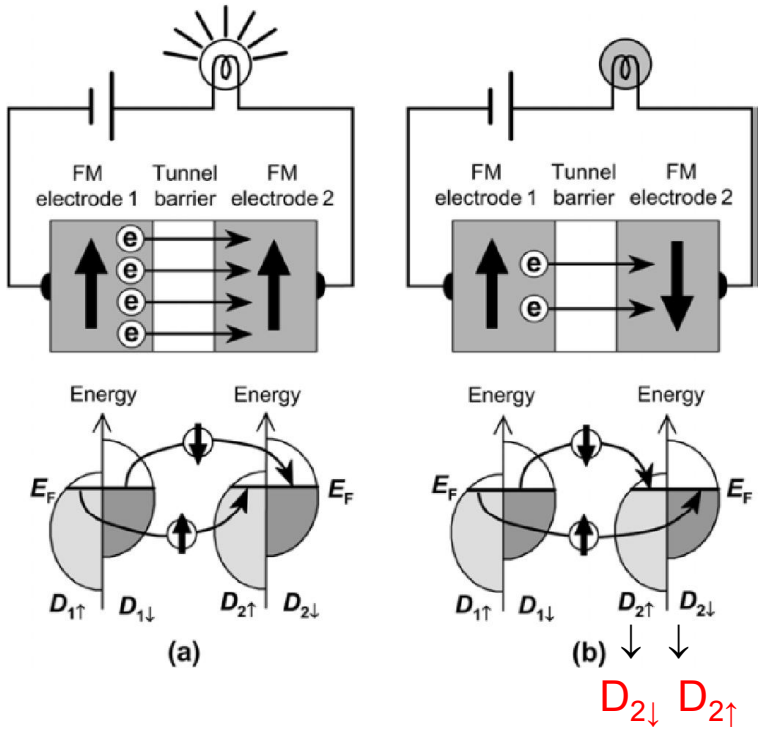

SPIN-POLARIZED TUNNELING

Schematic illustration of the TMR effect in a MTJ.
(a) Magnetizations in the two electrodes are aligned parallel (P).
(b) Magnetizations are aligned antiparallel (AP).
D1↑ and D1↓,respectively, denote the density of states at EF for the majority-spin and minority-spin bands in electrode 1, and D2↑ and D2↓ are respectively those for electrode 2.

$\Rightarrow$ $D_{\uparrow} - D_{\downarrow}$ >> than what is shown for high polarization materials!!!

In an MTJ, the resistance of the junction depends on the relative orientation of the magnetization vectors M in the two electrodes.

When the M's are parallel, tunneling probability is maximized because electrons from those states with a large density of states can tunnel into the same states in the other electrode. When the magnetization vectors are antiparallel, there will be a mismatch between the tunneling states on each side of the junction. This leads to a diminished tunneling probability, hence, a larger resistance.

Tunnel Magnetoresistance (TMR)

Assuming no spin-flip scattering, the MR ratio between the two configurations is given by,
$(\Delta R/R_P) = (R_{AP}-R_P)/R_P = 2P^2/(1-P^2)$, where R_P/R_{AP} is the resistance for the P/AP configuration & $P = (D_\uparrow - D_\downarrow)/(D_\uparrow + D_\downarrow)$ = spin-polarization parameter of the magnetic electrodes. A half-metal corresponds to P = 1.

Gang Mao, Gupta, el al. at Brown & IBM obtained below 200 Oe a GMR of 250 % in MTJ's with electrodes made of epitaxial films of doped half-metallic manganite $La_{0.67}Sr_{033}MnO_3$ (LSMO) and insulating barrier of $SrTiO_3$ using self-aligned lithographic process to pattern the junctions to micron size. They confirmed the spin-polarized tunneling as the active mechanism with P ~ 0.75. The low saturation field comes from the fact that manganites are magnetically soft, having a coercive field as small as 10 Oe. They have also made polycrystalline films with a large number of the grain boundaries and observed large MR at low fields. Here the mechanism has been attributed to the spin-dependent scattering across the grain boundaries that serve to pin the magnetic domain walls.

GANG MAO, A. GUPTA, X. W. LI, G. Q. GONG, and J. Z. SUN, Mat. Res. Soc. Symp. Proc. Vol. 494 (1998)
S. Yuasa and D. D. Djayaprawira, J. Phys. D: Appl. Phys. 40, R337–R354 (2007).

Hall effect in 5 layers of TiN/Ni nanocrystals

Hysteresis loop

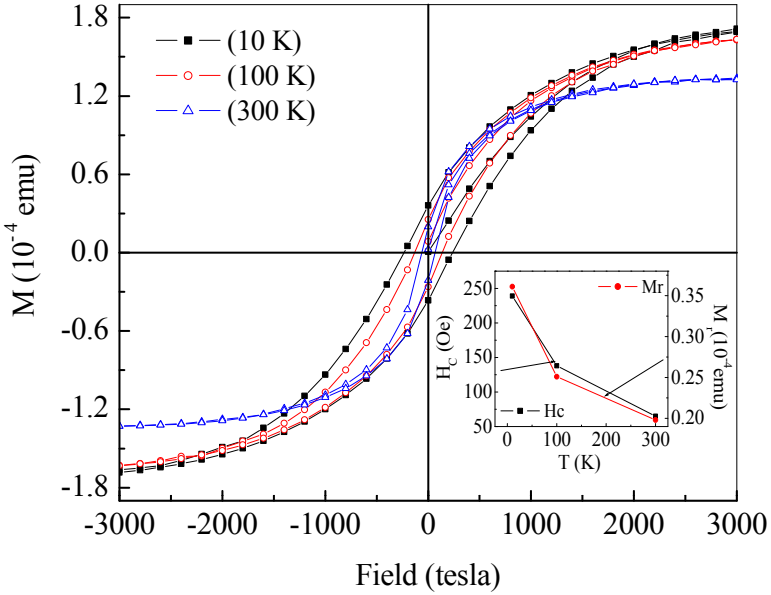

Using IITK-made PPMS

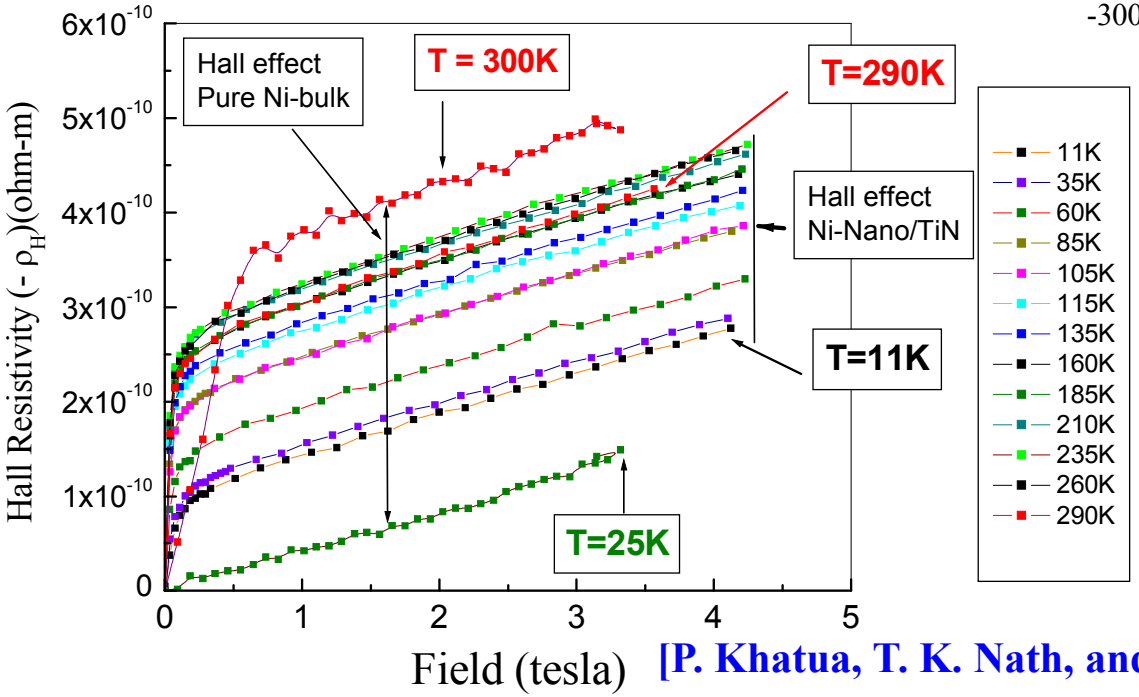

Hall effect

- ρ_H is negative at all temperatures from 11 to 290 K.

[P. Khatua, T. K. Nath, and AKM, Phys. Rev. B 73, 064408 (2006).]

Colossal Magnetoresistance (CMR)

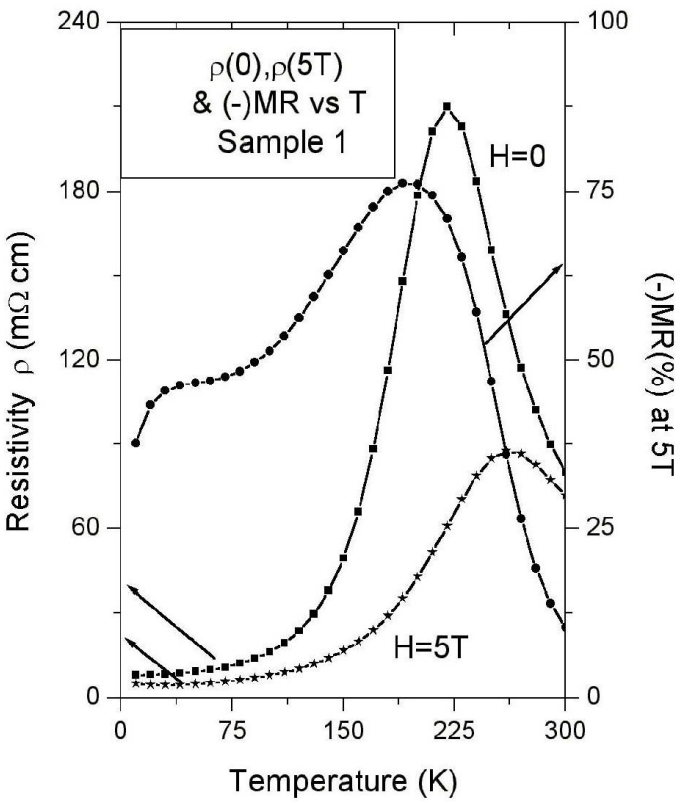

$La_{0.7}Ca_{0.3}MnO_3$ thin films

- Another class of materials, the rare-earth manganite oxides, $La_{1-x}D_xMnO_3$ (D=Sr, Ca, etc.), show Colossal Magnetoresistance effect (CMR) due to simultaneous occurrence of metal-insulator (M-I) and FM-PM phase transitions with a very large negative MR near T_C when subjected to a tesla-scale magnetic field.
- The **double-exchange model of Zener** and a strong e-ph interaction from the **Jahn-Teller splitting** of Mn d levels explain most of their magnetotransport properties.
- Though fundamentally interesting, the CMR effect, achieved only at large fields and below 300 K, poses severe technological challenges to potential applications in magnetoelectronic devices, where low field sensitivity is crucial.

D. Kumar, J. Sankar, J. Narayan, Rajiv K. Singh, and AKM, Phys. Rev. B 65, 094407 (2002).

Colossal Magnetoresistance (CMR)

Structure

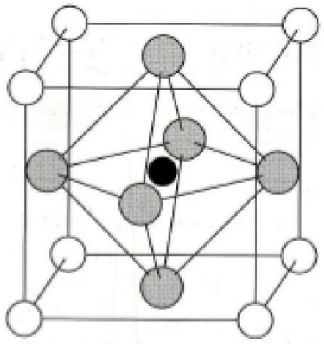

Figure 11.22 The perovskite structure. The small cation (in black) is surrounded by an octahedron of oxygen anions (in gray). The large cations (white) occupy the unit cell corners. XXXX

Phase Diagram

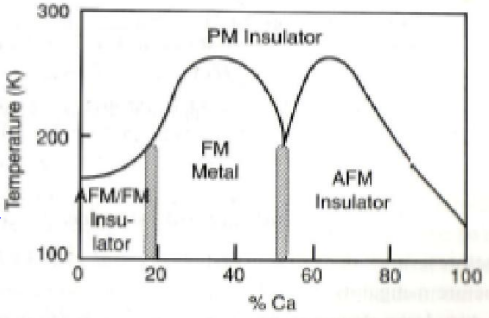

Figure 11.23 The phase diagram of $La_{1-x}Ca_xMnO_3$. From Ref. 56. Copyright (1995) by the American Physical Society. XXXX

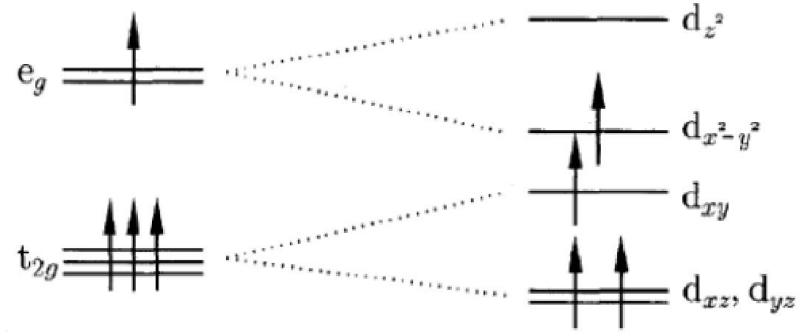

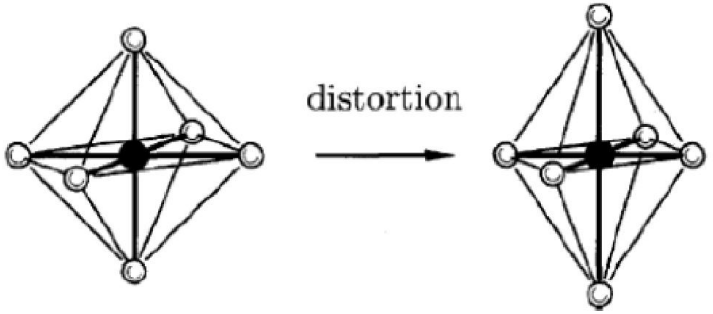

Jahn-Teller effect

Figure 6. The Jahn-Teller effect for $Mn^{3+}(3d^4)$. An octahedral complex (left) can distort (right), thus splitting the t_{2g} and e_g levels. The distortion lowers the energy because the singly occupied e_g level is lowered in energy. The saving in energy from the lowering of the d_{xz} and d_{yz} levels is exactly balanced by the raising of the d_{xy} level.

Double exchange

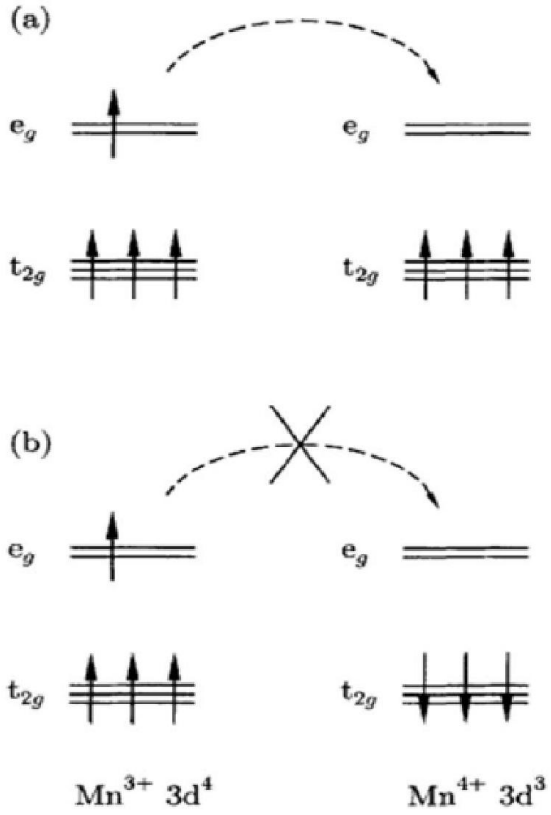

Figure 4. Double exchange mechanism gives ferromagnetic coupling between Mn^{3+} and Mn^{4+} ions participating in electron transfer. Intersite exchange interaction favors hopping if (a) spins on neighboring ions are ferromagnetically aligned and not if (b) neighboring ions are antiferromagnetically aligned.

Colossal Magnetoresistance (CMR)

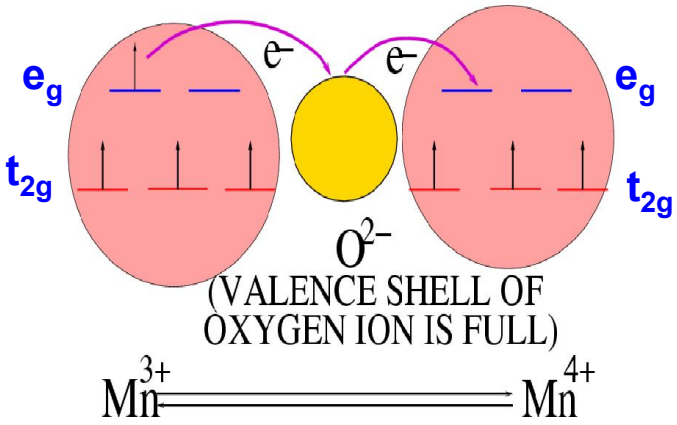

The origin of CMR stems from the strong interplay among the electronic structure, magnetism, and lattice dynamics in manganites. Doping of divalent Ca or Sr impurities into trivalent La sites create mixed valence states of Mn^{3+} (fraction: l-x) and Mn^{4+} (fraction: x). $Mn^{4+}(3d^3)$ has a localized spin of S = 3/2 from the low-lying t_{2g} 3 orbitals, whereas the e_g obitals are empty. Mn^{3+} $(3d^4)$ has an extra electron in the e_g orbital, which can hop into the neighboring Mn^{4+} sites (Double Exchange). The spin of this conducting electron is aligned with the local spin (S = 3/2) in the t_{2g} 3 orbitals of Mn^{3+} due to strong Hund's coupling. When the manganite becomes ferromagnetic, the electrons in the e_g orbitals are fully spin-polarized. The band structure is such that all the conduction electrons are in the majority band. This kind of metal with empty minority band is generally called a half-metal and so manganites have naturally become a good candidate for the study of spin-polarized transport.

Colossal Magnetoresistance (CMR)

Double exchange

Zener (1951) offered an explanation that remains at the core of our understanding of magnetic oxides. In doped manganese oxides, the two configurations

$$\psi_1: Mn^{3+}O_2^{-2}Mn^{4+} \text{ and } \psi_2 : Mn^{4+}O_2^{-2}Mn^{3+}$$

are degenerate and are connected by the so-called double-exchange matrix element. This matrix element arises via the transfer of an electron from Mn^{3+} to the central O_2^{-2} simultaneous with transfer from O_2^{-2} to Mn^{4+}. The degeneracy of ψ_1 and ψ_2 , a consequence of the two valencies of the Mn ions,makes this process fundamentally different from the above conventional superexchange. Because of strong Hund's coupling, the transfer-matrix element has finite value only when the core spins of the Mn ions are aligned ferromagnetically. The coupling of degenerate states lifts the degeneracy, and the system resonates between ψ_1 and ψ_2 if the core spins are parallel, leading to a ferromagnetic, conducting ground state. The splitting of the degenerate levels is $k_B T_C$ and, using classical arguments, predicts the electrical conductivity to be $s' \times e^2 a h T_C / T$ where 'a' is the Mn-Mn distance and x, the Mn^{4+} fraction.

Nano-magnetism

➢ Recording Media

- A good medium must have high M_r and H_C .
- In the year 2000 areal storage density of 65 Gbit/sq. inch was obtained in CoCrPtTa deposited on Cr thin films/$Cr_{80}Mo_{20}$ alloy.
- To achieve still higher density like 400Gbit/sq. inch it is necessary to use patterned medium instead of a continuous one. This is an assembly of nano-scale magnetically independent dots, each dot representing one bit of information.
- Some techniques are self-organization of nano-particles, nano-imprints or local ion irradiation.
- Problem of reducing magnetic particle size is the so-called “Superparamagnetic limit”.

What is Superparamagnetism ???

Superparamagnetism

In magnetic materials, the most common anisotropy is the "magnetocrystalline" anisotropy caused by the spin-orbit interaction.

It is easier to magnetize along certain crystallographic directions.

The energy of a ferromagnetic particle (many atoms) with uniaxial anisotropy constant K_1(energy/vol.) and magnetic moment μ making an angle θ with **H** || z-axis is , $\mathcal{E} = K_1 V \sin^2\theta - \mu H \cos\theta$,V being the volume of the particle. This has two minima at

at $\theta = 0$ and π with energies $\mathcal{E}_1 = -\mu H$ and $\mathcal{E}_2 = +\mu H$

and a barrier in between. Assuming that M of the particles spend almost all their time in one of the minima, the no. of particles jumping from min. 1 to min. 2 is a function of the barrier height $\varepsilon_m - \varepsilon_1$, where ε_m = energy of the maximum.

To get ε_m , put $\partial\varepsilon/\partial\theta = 0 = \sin\theta\,(2K_1 V \cos\theta + \mu H)$.

Superparamagnetism

There are several types of anisotropies in magnetic materials, the most common is the "magnetocrystalline" anisotropy caused by the spin-orbit interaction in a ferromagnet. It is easier to magnetize along certain crystallographic directions. This energy term is direction dependent**.** The energy of a ferromagnetic particle (many atoms) with uniaxial anisotropy constant K_1(energy/vol.) and magnetic moment μ making an angle θ with **H** || z-axis is $\mathcal{E} = K_1 V \sin^2\theta - \mu H \cos\theta$, V being the volume of the particle. This has two minima at $\theta = 0$ and π with energies $\mathcal{E}_1 = -\mu H$ and $\mathcal{E}_2 = +\mu H$ and a barrier in between.

Assuming that M of the particles spend almost all their time in one of the minima, the no. of particles jumping from min. 1 to min. 2 is a function of the barrier height $\varepsilon_m - \varepsilon_1$, where ε_m = energy of the maximum. To get ε_m , put $\partial\varepsilon/\partial\theta = 0 = \sin\theta\,(2K_1 V \cos\theta + \mu H)$.

Superparamagnetism

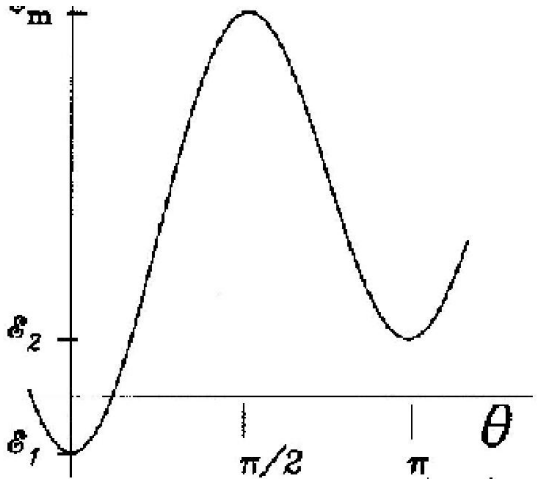

- $\sin\theta = 0$ gives two minima at $\theta = 0$ and π.
- The other solution gives the maximum.

$$\mathcal{E}_m = K_1 V + \frac{\mu^2 H^2}{4K_1 V} = K_1 V \left[1 + \left(\frac{H M_s}{2K_1}\right)^2\right] ,$$

where $\mu = V M$ and $|M| = M_S$.

The frequency of jump from min. 1 to min.2 is

$$\nu_{12} = c_{12} e^{-\beta(\mathcal{E}_m - \mathcal{E}_1)} = c_{12} e^{-\beta K_1 V (1 + H/H_K)^2}$$

where $H_K = \frac{2K_1 V}{\mu} = \frac{2K_1}{M_s}$.

Converting to relaxation time for H = 0 gives

$$\frac{1}{\tau} = f_0 e^{-\alpha} \quad \text{with} \quad \alpha = \frac{K_1 V}{k_B T}$$ & K_1V = Energy barrier.

Neel's estimate of f_0 was 10^9 s^{-1}. Current values are ~ 10^{10} s^{-1}.

Superparamagnetism

Material	R (Å)	τ (s)
Cobalt	44	6×10^5
	36	0.1
Iron	140	1.5×10^5
	115	0.07
Nickel	85	10×10^5
	75	10

- This table shows prominently the exponential behaviour of τ (R). For , say, Ni, τ increases by 5 orders of magnitude as R changes from 75 to 85 Å.
- If $\tau >> \tau_{exp}$, experimental time scale, no change of M could be observed during τ_{exp} ➔ " Stable ferromagnetism".

- If $\tau << \tau_{exp}$, M will flip many many times during τ_{exp} & average M will be 0. Thus there is a loss of " Stable ferromagnetism" since the relaxation time, τ, is too small.

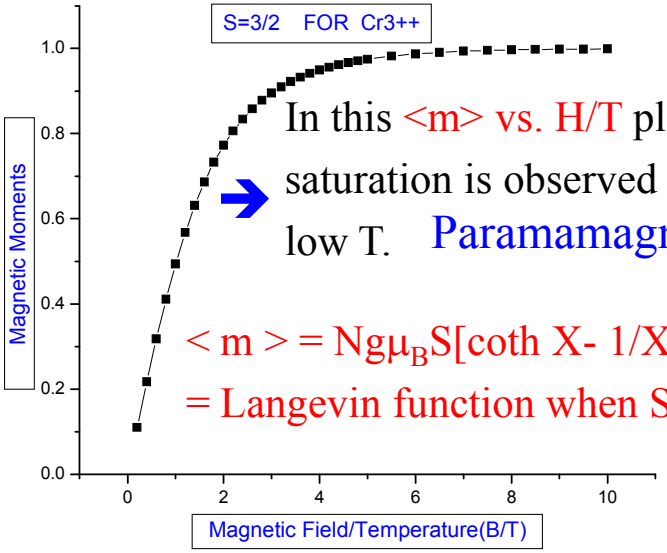

In this <m> vs. H/T plot paramagnetic saturation is observed only at very high H & low T. ➔ Paramamagnetism

$< m > = Ng\mu_B S[\coth X - 1/X] = L(X)$

= Langevin function when $S \rightarrow \infty$, $X = Sx$.

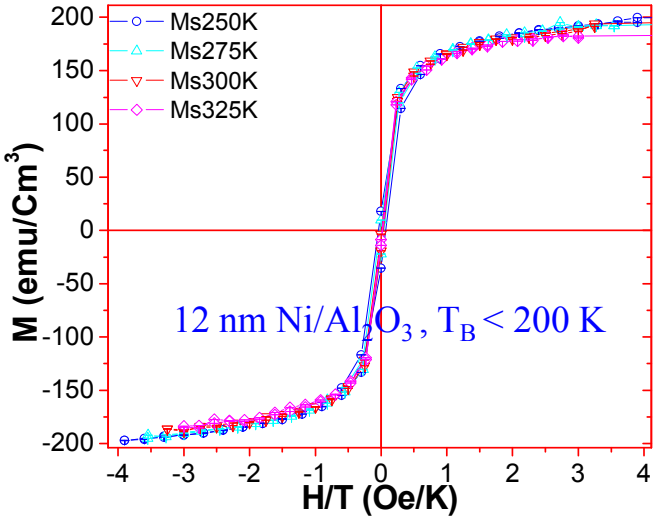

<M> vs. H/T curves coalesce to one but no hysteresis.

Superparamagnetism

- But in a field **H** , **M** will behave as a paramagnet as shown in <m> vs. H/T plot of last page with easy saturation when all the particles align at a much lower field & higher temperature since S in Langevin function (~ SH/T) is now 10^3 - 10^4. This is "Superparamagnetism"(SPM) --- "super" meaning "very high" as in "Superconductor".

- Transition from stable FM to SPM shifts to smaller particle size when T is decreased since τ is a function of V/T. The temperature, T_B at which $\tau \sim \tau_{exp}$, is called the "Blocking temperature". Above T_B, SPM with all M vs. H/T curves coalesce to one but no hysteresis (see earlier slide). Below T_B, it is in a "blocked" (FM) state with hysteretic M_r and H_C .

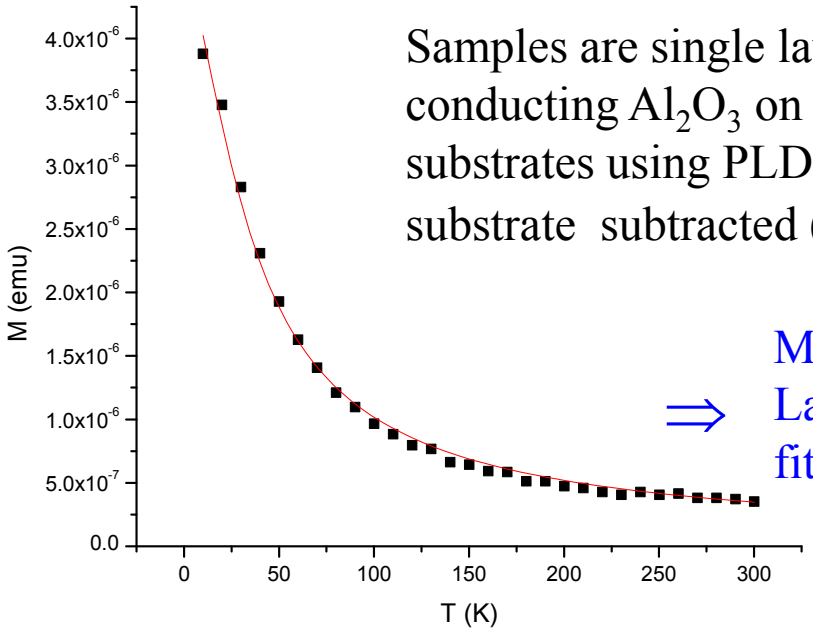

Samples are single layers of Ni nanoparticles with non-conducting Al_2O_3 on both sides deposited on both Si/Sapphire substrates using PLD technique. Diamagnetic contribution of substrate subtracted (typically $\chi = -2 \times 10^{-4}$ emu/tesla).

$\Rightarrow$ M (T) at H = 200 Oe for 6 nm Ni sample. Langevin/Brillouin function $M = M_0$ (cothx-1/x) fits very well with $\mu = 2700\ \mu_B$ where $x = \mu H/k_B T$.

Superparamagnetism

Ni nanocrystals in Alumina & TiN matrices

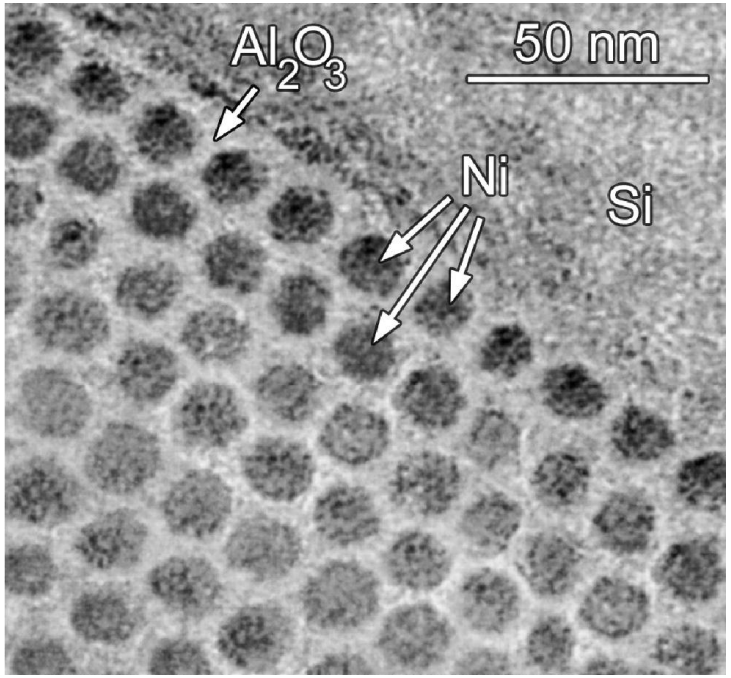

Self-assembled nickel nano particles in alumina thin film matrix with uniform size distribution averaging (13.2 ± 0.3) nm.

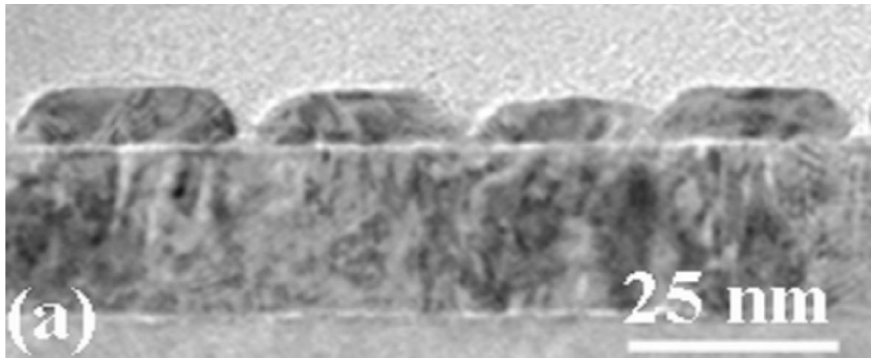

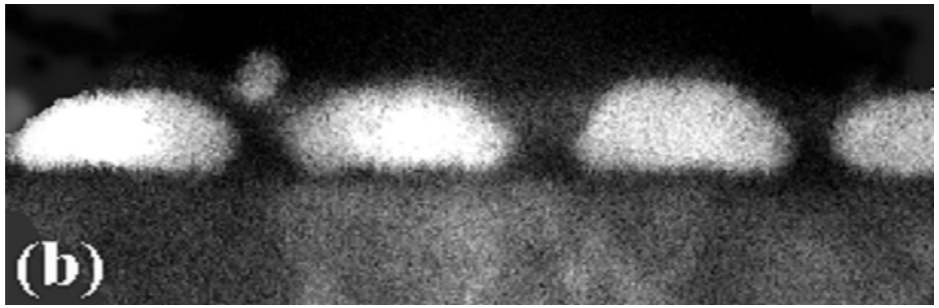

Images of truncated pyramidal shaped nickel islands on TiN:
(a) low-magnification TEM, and
(b) HRSTEM Z-contrast image.

Nano-magnetic Systems

Sample details

Five alternating layers of Ni (nano dots) and TiN (metallic matrix) were deposited on Si using PLD method:

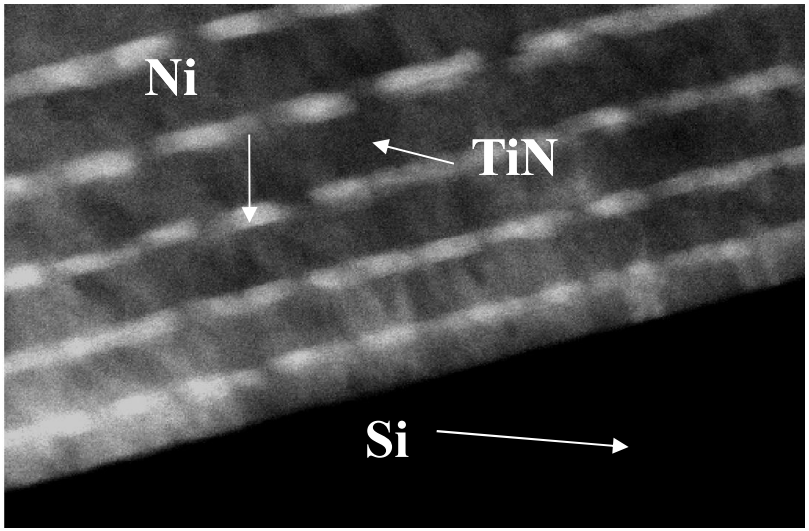

STEM-Z image of Ni nanoparticles embedded in TiN metal matrix.

- Base pressure = 5×10^{-7} Torr
- Substrate temperature = 600 ˚C
- Energy density and repeatition rate of the laser beam are 2J/cm^2 and 10Hz.

Why TiN?

Chemical stability, hardness, acts as diffusion barrier for both Ni and Si, high electrical conductivity, grows as a buffer layer epitaxially on Si.

D. Kumar, H. Zhou, T. K. Nath, Alex V. Kvit, and J. Narayan, Appl. Phys. Lett. 79, 2817 (2001).


Thanks.....